Contrib Mineral Petrol (2005) 149: 556–575
DOI 10.1007/s00410-005-0664-9

ORIGINAL PAPER

Shichun Huang · Frederick A. Frey

Recycled oceanic crust in the Hawaiian Plume: evidence from temporal geochemical variations within the Koolau Shield

Received: 22 September 2004 / Accepted: 28 February 2005 / Published online: 21 May 2005

Abstract The subaerial surface of Koolau volcano is composed of lavas that define the distinctive endmember composition for Hawaiian shield lavas, known as the Koolau component, now designated as the Makapuu-stage. The geochemical characteristics of lavas recovered by the Koolau Scientific Drilling Project (KSDP) show that this distinctive composition forms a <300-m thick veneer. Below this veneer, from ~300m to 470 m below sea level, Koolau shield lavas transition to a composition similar to Mauna Loa lavas, now designated as the Kalihi-stage. This transition was gradual, occurring over >80 ka; therefore it was not caused by an abrupt event, such as a landslide. Among all Koolau shield lavas, there are correlations between radiogenic isotopic ratios of Sr, Nd and Pb and compositional characteristics, such as SiO_2 content (adjusted to be in equilibrium with Fo_{90} olivine), Sr/Nb, La/Nb and Th/La. These long-term compositional and isotopic trends show that as the shield aged, there was an increasing role for an ancient recycled marine sediment component ($<3\%$ of the source) accompanied by up to 20% SiO_2-rich dacitic melt. This melt was generated by partial melting of garnet pyroxenite, probably kilometers in size, that formed from recycled basaltic oceanic crust. In detail, time series analyses of depth profiles of Al_2O_3/CaO, Sr/Nb, La/Nb and Th/La in the KSDP drill core show correlations among these ratios indicating that recycled oceanic crust contributed episodically, ~29 ka period, to the magma source during the prolonged transition from Kalihi- to Makapuu-stage lava compositions. The long-term geochemical trends show that recycled oceanic crust was increasingly important as the Koolau shield moved away from the plume and encountered lower temperature.

Communicated by T.L. Grove

S. Huang (✉) · F. A. Frey (✉)
Department of Earth, Atmospheric and Planetary Sciences,
Massachusetts Institute of Technology,
54-1210 EAPS 77 Massachusetts Ave, 02139 MA, Cambridge
E-mail: huangs@mit.edu
Tel.: +617-253-2869
Fax: +617-253-7102
E-mail: fafrey@mit.edu

Introduction

Although shield-stage lavas of Hawaiian volcanoes are derived from the Hawaiian hotspot, commonly inferred to be a mantle plume, many Hawaiian shields are distinct from one another in major and trace element abundances, as well as isotopic ratios (e.g., Frey and Rhodes 1993; Frey et al. 1994; Hauri 1996; Lassiter and Hauri, 1998). Some of these geochemical differences may be related to melting processes, but there is no doubt that the mantle source for Hawaiian shield lavas is geochemically heterogeneous. Compositions of lavas collected from subaerial exposures of the Koolau shield on Oahu define an extreme endmember. They are characterized by relatively high SiO_2 content, SiO_2/total iron, Al_2O_3/CaO, La/Nb, Sr/Nb, $^{87}Sr/^{86}Sr$, $^{187}Os/^{188}Os$, $\delta^{18}O$ and low total iron and CaO contents, $^{143}Nd/^{144}Nd$, $^{176}Hf/^{177}Hf$ and $^{206}Pb/^{204}Pb$ (e.g., Frey et al. 1994; Roden et al. 1994; Lassiter and Hauri 1998; Blichert-Toft et al. 1999). These geochemical characteristics have provided support for recycled oceanic crust, including sediments, in the source of Koolau lavas.

It is also well established that there are important temporal geochemical changes within individual Hawaiian shields. At some shields there are large variations, e.g., Mauna Loa (Rhodes and Hart 1995; Kurz et al. 1995), whereas at others, such as Mauna Kea, the temporal changes are relatively subtle (e.g., *Special Section of Hawaii Scientific Drilling Project in J. Geophys. Res., 1996 Vol. 101, pp 11593–11864; Theme of Hawaii Scientific Drilling Project in Geochem. Geophys. Geosyst. 2003*). Hence, an important question is – Does the entire Koolau shield have the end-member geochemical characteristics manifested by the subaerially

exposed lavas? Studies of lavas recovered from a highway (H3) tunnel (Jackson et al. 1999) and from the submarine landslide blocks (Shinozaki et al. 2002; Tanaka et al. 2002) indicate that the geochemical characteristics of older Koolau lavas may not be similar to the surface Koolau lavas. Specifically, Tanaka et al. (2002) argue for a temporal transition from Mauna Kea-like to Mauna Loa-like to Koolau-like with decreasing age. However, determining the origin and relative age of lavas from landslide blocks is difficult. A more direct approach to determining temporal geochemical variations in Koolau shield lavas is drilling and coring. This goal was achieved by the Koolau Scientific Drilling Project (KSDP) which deepened and cored a ~351 m water well to a depth of ~679 m (Haskins and Garcia 2004). The upper 351 m were rotary drilled and only rock chips are available, whereas nearly continuous core was recovered from the lower 328 m using a diamond drill bit. This core samples 103 subaerially erupted lava flows and one sedimentary unit. Based on petrography and compositions of whole-rocks and glasses, Haskins and Garcia (2004) conclude that the distinctive geochemical features of uppermost Koolau lavas (hereafter referenced as Makapuu-stage lavas) "form a veneer only 175–250 m thick at the drill site". This veneer overlies lavas with Mauna Loa-like major element compositions which Haskins and Garcia (2004) define as the Kalihi-stage of the Koolau shield.

As part of a team effort studying the KSDP core, we report 26 trace element abundances in 91 KSDP core samples (Table 1) analyzed by inductively coupled plasma mass spectrometry (ICP-MS); see Appendix A2 of Huang and Frey (2003) for procedures and discussion of accuracy and precision. We use these data, in conjunction with major element compositions and Nd–Hf–Pb isotopic ratios (Haskins and Garcia 2004; Fekiacova et al. in preparation; Salters et al., in preparation), to understand the temporal evolution of Koolau shield lavas.

Makapuu-stage lavas have been studied by Frey et al. (1994), who used X-ray fluorescence (XRF) and instrumental neutron activation (INAA) to obtain trace element data. In order to minimize bias caused by using different analytical methods, we reanalyzed by ICP-MS 15 Makapuu-stage lavas which have been analyzed for Sr–Nd–Pb isotopic ratios (Roden et al. 1994) and major and trace elements (Frey et al. 1994) (Table 2)

Results: incompatible elements

Abundances of incompatible elements that are immobile during alteration, such as Nb and La, are positively correlated with Th abundance for both Makapuu-stage lavas and Kalihi-stage lavas (Fig. 1a, c). Sr and Rb abundances are generally correlated with Th abundance; however, these trends are more scattered (Fig. 1b, d). Some of this scatter, e.g., to relatively low Rb abundance, is caused by altered samples. There are significant differences between Makapuu-stage and Kalihi-stage lavas; at a given Th abundance Makapuu-stage lavas have higher La and Sr abundances than Kalihi-stage lavas (Fig. 1a, c).

Figure. 2 shows the primitive mantle normalized trace element abundances of Makapuu-stage and Kalihi-stage lavas. Both lava suites have been adjusted to be in equilibrium with mantle olivine composition (Fo_{90}) to minimize the effect of crystal fractionation. The most obvious difference between the two lava suites is the relative Sr enrichment in the Makapuu-stage lavas. Since only relatively unaltered lavas are plotted, the enrichment of Sr in Makapuu-stage lavas is not a result of post-magmatic alteration. In contrast to the large variations in highly incompatible elements, abundances of heavy rare earth elements are nearly constant in both Makapuu-stage and Kalihi-stage lavas (Fig. 2).

Discussion

The Transition from Makapuu-Stage to Kalihi-Stage Lavas: Constraints from the KSDP Core

Haskins and Garcia (2004: Fig. 10) used Al_2O_3/CaO to define a change from the Makapuu-stage ($Al_2O_3/CaO > 1.45$) to Kalihi-stage ($Al_2O_3/CaO2O_3/CaO$ within the KSDP drill core (Fig. 3a). Within the upper part of the KSDP core, at a depth level inferred to be Kalihi-stage lavas, there are two groups of lavas which have Al_2O_3/CaO near the boundary between Makapuu- and Kalihi-stage lavas. Units 4, 5, 6 and 9, 10, 12 have $Al_2O_3/CaO = 1.42$ to 1.44 (Fig. 3a). Deeper in the core, Units 70, 85 and 88 have Al_2O_3/CaO of 1.43, 1.45 and 1.54, respectively. Units 85 and 88 are altered lavas; i.e., among Kalihi-Stage lavas, Unit 88 has the highest Loss on Ignition (L.O.I. = 3.65%), and Unit 85 has a L.O.I. of 2.89% (Table 4 of Haskins and Garcia 2004). Consequently, their high Al_2O_3/CaO may be a result of alteration.

The presence of orthopyroxene microphenocrysts is a petrographic characteristic of Makapuu-stage lavas (Frey et al. 1994), but orthopyroxene also occurs in KSDP cored lavas classified as Kalihi-stage lavas, that is, orthopyroxene is present in 6 of the uppermost 11 lava flows, including Units 9, 10 and 12 with high Al_2O_3/CaO, is absent in the underlying 42 lava flows, and is sporadically present in 13 of the lowermost 37 lava flows (Table 2 of Haskins and Garcia 2004).

Surface Koolau lavas, i.e., Makapuu-stage lavas, are distinguished from other Hawaiian shield lavas by their relatively high La/Nb and Sr/Nb (Fig. 11 of Frey et al. 1994; Fig. 13b of Huang and Frey 2003). A distinct difference between Makapuu-stage and Kalihi-stage lavas in La/Nb and Sr/Nb is apparent in Fig. 4a

Table 1 Trace element abundances (in ppm) in KSDP Lavas determined by ICP-MS

KSDP unit	Elev. (m)	Rock type	Sc	Rb	Sr	Y	Zr	Nb	Ba	La	Ce	Pr	Nd	Sm	Eu	Gd	Tb	Dy	Ho	Er	Tm	Yb	Lu	Hf	Ta	Pb	Th	U
1	−303.8	picrite	23.3	3.16	249	19.4	95	7.06	69.1	7.18	17.6	2.68	12.8	3.56	1.22	3.87	0.623	3.55	0.698	1.78	0.259	1.49	0.216	2.47	0.474	0.976	0.497	0.136
2	−308.4	picrite	22.2	1.85	225	17.3	85	6.15	60.7	6.17	15.3	2.36	11.2	3.15	1.09	3.45	0.555	3.10	0.617	1.55	0.227	1.34	0.190	2.19	0.410	1.14	0.434	0.123
3	−308.9	picrite	22.6	3.44	250	19.9	98	7.14	66.1	7.53	18.9	2.78	13.1	3.72	1.31	4.05	0.653	3.69	0.705	1.91	0.261	1.54	0.218	2.63	0.489	1.12	0.524	0.152
4	−312.3	ol basalt	25.8	2.38	318	22.8	121	7.61	73.8	8.31	20.6	3.23	15.4	4.40	1.58	4.73	0.755	4.20	0.814	2.07	0.295	1.73	0.246	3.05	0.520	0.936	0.573	0.165
5	−314.4	picrite	22.4	2.71	259	18.9	98	6.29	72.9	6.68	17.4	2.55	12.6	3.60	1.29	3.93	0.636	3.56	0.689	1.78	0.254	1.50	0.210	2.56	0.422	0.828	0.465	0.143
6	−316.6	picrite	21.0	3.55	261	18.9	97	6.28	66.1	6.81	16.8	2.66	12.8	3.66	1.29	3.90	0.623	3.50	0.678	1.75	0.241	1.44	0.203	2.53	0.430	0.795	0.455	0.140
7	−325.0	ol basalt	27.9	4.66	301	23.9	126	8.35	76.6	8.50	21.4	3.36	16.0	4.52	1.59	4.80	0.792	4.33	0.838	2.16	0.301	1.78	0.247	3.25	0.560	1.58	0.571	0.171
8	−329.0	ol basalt	26.6	5.15	304	24.6	125	8.52	79.1	8.78	21.9	3.43	16.4	4.59	1.59	4.98	0.796	4.48	0.868	2.22	0.308	1.80	0.256	3.21	0.558	1.04	0.555	0.173
9	−332.4	ol basalt	26.9	3.46	267	23.4	104	6.85	59.0	7.04	17.3	2.72	13.3	3.96	1.43	4.44	0.726	4.19	0.830	2.12	0.300	1.79	0.257	2.74	0.465	0.744	0.465	0.146
10	−334.2	basalt	27.1	2.25	271	22.7	103	6.98	69.8	6.99	18.1	2.73	13.1	3.93	1.40	4.37	0.736	4.17	0.811	2.07	0.294	1.75	0.252	2.68	0.472	0.836	0.486	0.137
12	−336.0	basalt	26.2	3.59	274	23.3	108	7.27	67.7	7.13	17.9	2.76	13.4	4.00	1.42	4.45	0.728	4.14	0.814	2.08	0.300	1.74	0.248	2.77	0.477	1.06	0.467	0.138
13	−338.0	basalt	29.9	7.15	378	27.8	158	11.4	106	12.1	29.9	4.50	21.2	5.62	1.92	5.81	0.920	5.13	0.970	2.43	0.346	2.02	0.286	3.96	0.729	1.23	0.814	0.247
14	−341.9	ol basalt	30.2	7.03	371	27.1	151	10.8	101	11.7	30.1	4.29	20.4	5.46	1.86	5.70	0.886	4.93	0.957	2.47	0.341	1.99	0.278	3.84	0.701	1.23	0.794	0.241
15	−343.8	ol basalt	27.2	5.30	301	25.0	123	9.69	82.6	9.29	24.0	3.54	16.6	4.63	1.64	5.03	0.823	4.57	0.885	2.30	0.319	1.87	0.270	3.21	0.658	1.23	0.678	0.201
16	−345.5	basalt	30.0	6.79	380	27.5	156	11.9	107	11.9	30.4	4.43	21.6	5.63	1.92	5.82	0.931	5.13	0.990	2.52	0.351	2.01	0.283	4.00	0.801	1.30	0.793	0.243
17	−350.4	basalt	30.0	5.90	346	26.8	142	10.6	91.1	10.2	25.7	3.91	18.5	5.10	1.78	5.51	0.892	5.06	0.976	2.56	0.363	1.99	0.296	3.62	0.727	1.17	0.725	0.220
18	−355.6	ol basalt	29.7	5.95	375	28.1	155	11.4	93.0	11.2	28.8	4.25	20.4	5.56	1.91	5.82	0.935	5.14	0.987	2.52	0.350	2.02	0.287	3.87	0.748	1.17	0.785	0.228
19	−357.8	basalt	30.1	6.43	372	28.0	154	11.5	100	11.4	29.2	4.25	20.9	5.57	1.92	5.83	0.940	5.17	0.992	2.53	0.352	2.06	0.280	3.91	0.761	1.20	0.781	0.239
20	−359.2	picrite	26.1	5.63	312	23.3	129	10.2	90.4	9.74	24.4	3.64	17.1	4.61	1.56	4.84	0.775	4.37	0.818	2.16	0.293	1.71	0.241	3.32	0.671	1.06	0.692	0.203
21	−362.5	basalt	29.0	1.94	340	25.9	147	10.7	93.9	9.70	23.9	3.77	18.1	5.12	1.77	5.33	0.875	4.87	0.927	2.34	0.326	1.93	0.275	3.74	0.707	1.14	0.694	0.209
22	−363.9	basalt	30.0	5.13	346	25.7	135	9.68	82.2	9.10	24.4	3.56	17.5	4.90	1.69	5.14	0.825	4.67	0.910	2.33	0.331	1.90	0.275	3.43	0.643	0.993	0.635	0.198
23	−367.3	basalt	29.2	4.87	339	27.6	140	9.94	92.6	10.3	27.7	3.99	18.9	5.29	1.84	5.67	0.898	5.05	0.967	2.42	0.340	1.98	0.286	3.50	0.652	1.05	0.644	0.200
24	−370.6	basalt	28.5	4.68	330	26.1	133	9.54	81.2	9.62	25.1	3.71	17.8	5.03	1.78	5.40	0.879	4.88	0.948	2.41	0.332	1.94	0.274	3.51	0.640	0.957	0.635	0.197
25	−372.5	basalt	29.3	4.12	335	26.3	137	9.58	83.6	9.47	23.8	3.74	18.0	5.03	1.70	5.37	0.869	4.80	0.936	2.42	0.348	1.94	0.270	3.47	0.630	0.996	0.622	0.197
26	−376.1	basalt	28.8	5.44	336	26.9	141	10.1	82.9	10.2	26.3	4.02	18.9	5.24	1.83	5.63	0.904	5.02	0.954	2.48	0.331	1.99	0.286	3.70	0.673	1.36	0.668	0.210
27	−379.5	basalt	30.6	4.51	355	28.0	147	10.3	93.5	10.4	25.6	4.01	19.3	5.26	1.82	5.67	0.904	5.04	0.974	2.51	0.343	2.01	0.288	3.72	0.674	1.15	0.700	0.217
28	−379.8	basalt	29.7	6.16	342	26.7	145	10.3	92.9	10.2	26.2	3.98	19.1	5.30	1.81	5.60	0.893	5.01	0.967	2.49	0.351	2.02	0.289	3.73	0.682	1.08	0.731	0.230
29	−381.3	picrite	24.6	3.76	289	22.8	121	8.50	88.5	8.78	21.7	3.38	16.2	4.41	1.54	4.65	0.743	4.28	0.804	2.08	0.287	1.68	0.239	3.08	0.567	1.07	0.577	0.182
30	−383.0	basalt	27.6	4.58	306	25.2	128	9.07	93.9	9.36	23.1	3.61	17.2	4.73	1.57	5.06	0.805	4.62	0.878	2.28	0.317	1.84	0.263	3.24	0.590	1.13	0.669	0.209
31	−387.6	picrite	21.6	2.57	248	18.3	100	7.08	64.4	6.97	17.9	2.72	12.9	3.56	1.24	3.77	0.611	3.38	0.643	1.66	0.226	1.35	0.201	2.54	0.468	0.771	0.493	0.147
32	−388.2	picrite	26.7	2.49	298	22.5	123	8.73	83.2	8.71	21.9	3.42	16.4	4.49	1.54	4.72	0.762	4.24	0.816	2.10	0.292	1.69	0.239	3.15	0.575	0.989	0.602	0.170
33	−390.0	nd	30.8	4.22	325	26.5	143	10.4	95.8	9.46	24.4	3.78	17.9	5.00	1.76	5.36	0.860	4.87	0.929	2.43	0.337	2.00	0.280	3.63	0.679	1.20	0.700	0.210
34	−391.4	ol basalt	28.7	3.79	320	25.7	132	9.43	72.6	8.82	23.4	3.57	17.4	4.79	1.69	5.22	0.856	4.74	0.918	2.34	0.326	1.89	0.273	3.42	0.654	0.943	0.627	0.198
35	−392.0	ol basalt	30.4	3.31	323	28.3	141	10.2	87.0	9.50	25.5	3.78	18.1	5.13	1.77	5.49	0.897	5.09	0.985	2.61	0.354	2.08	0.293	3.67	0.672	1.08	0.674	0.219
36	−394.4	ol basalt	29.0	3.12	304	24.8	132	9.40	82.1	8.67	22.1	3.48	16.7	4.65	1.61	5.02	0.795	4.57	0.879	2.25	0.312	1.88	0.265	3.37	0.627	0.966	0.607	0.176
37	−395.8	basalt	30.8	4.68	327	27.0	140	10.2	90.4	9.52	24.3	3.80	18.0	5.06	1.77	5.48	0.880	4.89	0.962	2.43	0.346	1.99	0.286	3.61	0.676	1.22	0.658	0.194
38	−398.6	basalt	30.8	5.02	337	27.1	143	10.6	91.9	9.87	24.5	3.91	18.7	5.17	1.81	5.55	0.893	5.01	0.964	2.49	0.336	2.07	0.287	3.73	0.715	1.10	0.714	0.226
39	−403.9	basalt	31.6	4.74	348	28.2	152	11.1	90.6	9.87	27.0	3.93	19.4	5.42	1.87	5.74	0.917	5.16	1.01	2.57	0.358	2.09	0.294	3.82	0.731	1.14	0.708	0.221
40	−407.6	basalt	31.5	5.10	332	27.9	147	10.8	86.8	10.0	25.4	4.00	19.1	5.22	1.79	5.62	0.916	5.15	0.984	2.52	0.355	2.09	0.289	3.79	0.719	1.63	0.691	0.225
41	−408.8	basalt	31.6	4.70	339	29.8	153	11.0	97.9	10.6	25.5	4.21	20.2	5.63	1.87	6.04	0.974	5.47	1.07	2.75	0.390	2.21	0.316	3.98	0.739	1.12	0.725	0.228
44	−411.2	basalt	31.7	5.19	340	28.3	149	10.8	94.3	10.1	25.9	4.08	19.2	5.37	1.82	5.79	0.928	5.23	1.02	2.62	0.369	2.13	0.308	3.86	0.732	1.14	0.718	0.219
45	−412.3	basalt	27.9	4.80	308	24.9	131	9.25	83.5	9.10	23.1	3.63	17.5	4.72	1.64	5.08	0.819	4.59	0.890	2.30	0.322	1.86	0.257	3.38	0.636	1.01	0.615	0.190
46	−413.6	basalt	29.2	5.21	340	26.1	143	10.3	99.4	10.0	24.9	3.89	18.4	5.07	1.75	5.35	0.859	4.79	0.913	2.40	0.336	1.91	0.277	3.59	0.675	1.16	0.683	0.206
47	−418.8	basalt	31.1	5.37	342	26.5	142	10.3	86.8	9.99	25.0	3.87	18.5	5.10	1.70	5.31	0.856	4.78	0.929	2.42	0.337	1.95	0.277	3.61	0.677	1.10	0.673	0.204
48	−422.7	basalt	30.3	5.70	354	27.1	143	10.7	97.2	10.7	27.7	3.97	19.4	5.27	1.82	5.53	0.889	4.90	0.965	2.46	0.335	1.99	0.273	3.66	0.699	1.21	0.714	0.209
49	−426.1	basalt	32.0	4.71	329	26.1	136	9.77	78.0	9.00	23.3	3.60	17.4	4.84	1.68	5.17	0.839	4.71	0.898	2.33	0.323	1.88	0.278	3.50	0.645	0.979	0.652	0.195
50	−429.7	basalt	27.0	5.05	350	24.0	139	10.5	108	10.4	24.9	3.95	18.6	5.03	1.73	5.17	0.820	4.52	0.853	2.16	0.309	1.78	0.253	3.52	0.685	1.20	0.712	0.208
51	−433.4	basalt	31.6	4.94	350	26.9	143	9.71	90.8	9.77	24.2	3.87	18.6	5.14	1.81	5.51	0.884	4.90	0.937	2.44	0.328	1.96	0.279	3.60	0.647	1.02	0.642	0.199

52	−438.9	ol basalt	27.2	4.67	315	24.3	130	9.81	88.8	9.56	24.0	3.64	17.0	4.73	1.60	5.05	0.795	4.53	0.888	2.24	0.318	1.82	0.264	3.34	0.671	1.07	0.691	0.195
53	−440.4	ol basalt	25.8	5.37	299	23.0	124	9.57	93.4	8.84	22.3	3.31	15.9	4.41	1.55	4.74	0.753	4.30	0.831	2.12	0.295	1.75	0.249	3.21	0.640	1.10	0.656	0.193
54	−443.7	basalt	29.7	5.65	362	28.0	152	12.1	106	11.9	27.9	4.42	20.5	5.48	1.89	5.84	0.909	5.14	0.970	2.49	0.350	1.99	0.283	3.90	0.791	1.20	0.818	0.231
55	−445.7	basalt	31.9	3.17	372	27.5	158	12.8	109	11.1	28.4	4.38	20.7	5.62	1.96	5.89	0.928	5.20	0.987	2.44	0.356	2.06	0.290	4.01	0.828	1.23	0.867	0.221
56	−448.8	basalt	30.3	4.62	368	27.3	148	11.9	99.8	11.1	27.8	4.21	19.9	5.36	1.86	5.57	0.893	4.94	0.963	2.42	0.341	1.98	0.283	3.78	0.766	1.11	0.809	0.230
57	−453.2	basalt	29.5	5.06	353	27.4	153	12.2	108	11.1	27.9	4.28	20.2	5.45	1.90	5.68	0.930	5.03	0.972	2.50	0.342	2.02	0.285	3.90	0.799	1.16	0.830	0.221
59	−456.1	basalt	30.0	6.71	353	27.6	151	12.3	109	11.1	27.9	4.23	19.9	5.47	1.91	5.67	0.929	5.06	0.987	2.47	0.351	2.07	0.291	3.83	0.788	1.19	0.823	0.251
60	−464.6	basalt	30.6	2.78	366	30.3	165	13.6	115	12.2	29.7	4.54	21.5	5.77	1.96	6.20	0.998	5.50	1.07	2.75	0.382	2.18	0.315	4.10	0.878	1.19	0.876	0.191
61	−469.3	basalt	29.3	6.12	350	27.9	144	12.0	101	10.6	27.7	4.05	18.8	5.20	1.80	5.57	0.897	5.04	0.969	2.49	0.348	2.02	0.286	3.67	0.786	1.12	0.796	0.226
62	−476.4	basalt	28.9	5.71	324	25.2	130	11.04	97.3	9.61	25.0	3.65	17.1	4.66	1.63	5.02	0.817	4.61	0.889	2.33	0.323	1.85	0.261	3.27	0.700	0.991	0.698	0.199
63	−482.1	basalt	30.2	7.06	338	28.0	146	12.3	105	10.9	27.0	4.10	19.0	5.20	1.76	5.63	0.906	5.07	0.990	2.57	0.363	2.09	0.304	3.71	0.809	1.14	0.835	0.249
64	−493.4	ol basalt	26.3	3.45	252	21.6	99	6.87	61.3	6.59	17.3	2.57	12.6	3.69	1.32	4.13	0.669	3.92	0.748	2.01	0.276	1.63	0.236	2.56	0.463	0.802	0.444	0.132
65	−495.9	basalt	27.5	4.98	293	24.6	123	8.61	74.6	8.28	21.2	3.32	16.0	4.51	1.60	4.90	0.785	4.45	0.870	2.27	0.310	1.83	0.271	3.14	0.567	0.862	0.547	0.171
66	−506.9	basalt	29.3	5.73	318	25.0	131	9.98	82.7	9.20	23.3	3.60	17.1	4.68	1.64	5.11	0.804	4.54	0.892	2.27	0.324	1.88	0.267	3.37	0.656	1.05	0.630	0.191
67	−511.1	ol basalt	26.7	4.26	286	23.4	118	8.27	66.0	7.74	19.8	3.10	14.7	4.24	1.49	4.66	0.741	4.32	0.832	2.14	0.299	1.77	0.251	3.00	0.551	0.803	0.522	0.150
68	−514.2	ol basalt	28.1	3.53	316	24.5	128	8.86	73.8	8.78	22.5	3.41	16.1	4.54	1.58	5.00	0.800	4.56	0.869	2.26	0.314	1.79	0.255	3.26	0.599	0.951	0.607	0.172
69	−521.8	basalt	28.5	4.69	304	26.7	126	8.78	80.5	8.84	20.5	3.41	16.6	4.75	1.68	5.33	0.865	4.81	0.924	2.38	0.333	1.93	0.280	3.29	0.579	0.886	0.553	0.172
70	−526.0	basalt	29.0	2.70	300	24.1	124	8.61	185	8.20	19.0	3.16	15.3	4.48	1.60	4.84	0.787	4.40	0.848	2.15	0.305	1.77	0.248	3.15	0.555	0.885	0.552	0.190
71	−526.5	basalt	29.5	4.36	314	26.4	131	9.17	85.3	9.63	20.1	3.63	17.6	4.90	1.75	5.37	0.853	4.74	0.910	2.28	0.316	1.84	0.269	3.32	0.595	1.01	0.588	0.175
72	−533.7	basalt	30.0	3.81	322	27.0	135	9.65	80.9	9.34	23.9	3.61	17.5	4.82	1.70	5.36	0.880	4.85	0.951	2.45	0.339	1.94	0.279	3.41	0.648	1.06	0.608	0.182
73	−535.2	basalt	30.0	3.60	335	28.5	143	9.87	104	10.8	25.2	4.09	19.5	5.36	1.86	5.83	0.926	5.13	0.999	2.51	0.359	1.97	0.283	3.59	0.661	1.09	0.649	0.181
74	−537.9	basalt	29.8	4.11	320	26.5	133	9.24	95.6	9.20	22.6	3.50	17.0	4.76	1.69	5.21	0.839	4.69	0.907	2.34	0.314	1.88	0.264	3.45	0.613	1.00	0.638	0.172
75	−544.9	basalt	29.1	5.43	311	26.9	139	9.52	81.7	9.42	23.9	3.72	18.0	5.04	1.76	5.48	0.891	4.96	0.976	2.48	0.353	2.03	0.291	3.59	0.643	0.984	0.643	0.203
76	−550.3	basalt	32.0	2.40	305	24.8	140	9.68	84.0	8.72	22.4	3.74	18.3	5.13	1.82	5.38	0.849	4.70	0.898	2.23	0.307	1.78	0.255	3.64	0.669	0.948	0.609	0.186
81	−556.4	basalt	30.6	5.69	318	27.7	141	9.88	133	11.1	23.2	4.25	20.1	5.46	1.88	5.81	0.926	5.11	0.966	2.41	0.346	1.96	0.284	3.54	0.654	1.09	0.620	0.383
82	−558.7	basalt	31.8	2.38	325	29.5	144	10.2	73.3	10.5	24.9	4.11	19.7	5.38	1.88	5.88	0.952	5.27	1.03	2.63	0.374	2.14	0.300	3.72	0.684	1.00	0.648	0.180
83	−562.0	basalt	29.9	2.91	323	28.8	141	9.96	68.4	9.98	24.4	3.83	18.4	5.19	1.82	5.64	0.916	5.14	1.01	2.58	0.362	2.11	0.311	3.61	0.685	0.990	0.640	0.259
85	−564.8	ol basalt	29.0	3.12	283	27.1	135	11.3	114	11.5	26.8	4.22	19.6	5.09	1.73	5.47	0.858	4.93	0.946	2.48	0.344	1.97	0.286	3.36	0.734	1.59	0.748	0.213
87	−566.2	basalt	31.9	8.22	171	24.7	148	12.6	267	9.23	27.8	3.53	16.1	4.46	1.56	4.75	0.805	4.50	0.875	2.22	0.327	1.90	0.267	3.77	0.817	1.74	0.843	0.223
88	−569.4	ol basalt	24.9	2.42	212	21.4	104	8.68	81.6	8.72	21.1	3.15	14.5	3.92	1.37	4.24	0.685	3.87	0.753	1.95	0.274	1.64	0.233	2.73	0.589	0.947	0.631	0.117
91	−573.7	basalt	31.3	2.87	357	28.0	163	14.3	128	14.8	37.1	5.06	22.4	5.72	1.95	5.82	0.933	5.18	0.991	2.58	0.351	2.05	0.291	4.13	0.954	1.59	1.09	0.252
92	−581.7	picrite	21.5	2.10	191	18.7	94	7.89	207	7.40	18.0	2.71	12.8	3.46	1.16	3.77	0.604	3.43	0.650	1.66	0.231	1.33	0.189	2.38	0.531	1.08	0.486	0.122
93	−586.4	basalt	31.3	2.16	324	27.4	140	9.97	90.0	9.28	24.2	3.79	18.5	5.18	1.80	5.61	0.896	5.16	0.990	2.57	0.358	2.08	0.297	3.63	0.684	1.14	0.629	0.186
94	−590.4	basalt	30.3	1.44	330	27.3	129	8.86	68.0	9.04	22.5	3.55	17.3	4.88	1.72	5.37	0.854	4.81	0.943	2.41	0.337	1.98	0.282	3.30	0.604	1.05	0.544	0.157
95	−593.7	basalt	29.9	1.75	317	25.5	129	9.10	64.6	8.62	21.9	3.47	16.8	4.79	1.69	5.18	0.862	4.76	0.917	2.33	0.325	1.95	0.275	3.33	0.612	0.882	0.572	0.168
96	−596.0	basalt	30.3	1.40	316	24.1	116	8.23	64.3	7.92	19.8	3.14	15.3	4.34	1.55	4.70	0.762	4.27	0.832	2.13	0.309	1.79	0.256	2.99	0.545	1.12	0.510	0.160
97	−597.7	picrite	27.3	2.24	236	23.5	121	9.91	84.2	8.62	22.9	3.37	16.2	4.43	1.54	4.82	0.777	4.28	0.830	2.14	0.294	1.72	0.241	3.20	0.671	0.872	0.602	0.171
98	−600.3	basalt	31.8	2.07	294	27.4	134	10.8	83.9	9.05	23.4	3.65	17.5	4.95	1.75	5.51	0.891	5.01	0.989	2.51	0.359	2.06	0.292	3.54	0.720	0.989	0.638	0.158
100	−606.3	basalt	32.6	3.70	308	28.3	141	10.4	64.7	9.22	23.9	3.73	17.8	5.02	1.78	5.54	0.911	5.06	1.00	2.59	0.361	2.05	0.294	3.61	0.684	1.08	0.668	0.220
101	−622.3	basalt	30.6	3.03	295	24.0	120	8.97	49.5	8.23	21.3	3.29	15.7	4.23	1.48	4.72	0.752	4.33	0.841	2.19	0.305	1.74	0.254	3.05	0.607	0.835	0.539	0.162
102	−625.5	ol basalt	30.8	3.86	289	25.3	124	9.66	60.3	8.69	23.5	3.48	16.4	4.52	1.60	5.01	0.821	4.59	0.912	2.34	0.327	1.89	0.272	3.29	0.649	0.869	0.589	0.196
103	−627.8	basalt	32.5	3.32	311	28.0	135	10.3	66.3	9.53	25.7	3.70	17.5	4.87	1.68	5.38	0.892	4.96	0.982	2.53	0.354	2.07	0.293	3.47	0.686	0.925	0.641	0.203

Table 2 Trace Element Abundances (in ppm) in Makapuu-stage Lavas by ICP-MS

Sample[(1)]	Sc	Rb	Sr	Y	Zr	Nb	Ba	La	Ce	Pr	Nd	Sm	Eu	Tb	Dy	Ho	Er	Tm	Yb	Lu	Hf	Ta	Pb	Th	U
KOO-1	26.5	5.79	416	24.0	151	8.13	83.8	10.7	26.2	4.15	19.6	5.21	1.74	0.803	4.42	0.831	2.11	0.304	1.67	0.240	3.56	0.560	1.20	0.611	0.181
KOO-7	25.7	6.24	411	25.5	139	9.05	81.5	10.3	25.0	4.25	20.0	5.27	1.77	0.847	4.69	0.891	2.31	0.340	1.85	0.263	3.73	0.633	1.16	0.592	0.175
KOO-8	24.9	7.17	480	25.5	154	9.42	112	12.1	30.7	4.48	21.0	5.35	1.78	0.822	4.51	0.853	2.20	0.312	1.72	0.238	3.62	0.628	1.28	0.674	0.200
KOO-9	22.7	2.10	280	22.2	99	5.06	49.5	6.00	15.5	2.36	12.0	3.79	1.34	0.682	3.94	0.751	1.99	0.297	1.61	0.233	2.52	0.351	0.709	0.362	0.102
KOO-10	23.1	3.07	340	21.0	117	6.80	61.7	7.88	20.0	3.06	15.1	4.27	1.45	0.687	3.83	0.730	1.87	0.274	1.50	0.218	2.90	0.469	0.968	0.474	0.125
KOO-15	25.5	1.50	377	28.4	148	8.71	103	12.2	27.9	4.48	21.3	5.53	1.85	0.885	4.98	0.975	2.46	0.354	2.00	0.278	3.64	0.579	1.10	0.662	0.146
KOO-16	25.9	0.74	372	29.0	140	8.65	67.8	10.3	25.5	3.96	19.2	5.36	1.84	0.923	5.21	0.999	2.58	0.382	2.05	0.287	3.57	0.609	1.06	0.600	0.139
KOO-17A	19.2	0.23	276	19.5	101	5.64	40.3	7.72	18.2	2.85	13.3	3.39	1.13	0.538	3.00	0.597	1.55	0.225	1.23	0.173	2.36	0.387	0.743	0.388	0.075
KOO-20	28.8	7.26	454	26.4	171	10.7	110	13.2	33.3	4.90	23.2	5.96	1.95	0.916	5.03	0.954	2.42	0.350	1.96	0.275	4.09	0.713	1.43	0.756	0.194
KOO-26	26.6	1.87	345	25.0	115	6.80	61.8	8.44	20.6	3.14	15.2	4.29	1.49	0.747	4.29	0.841	2.16	0.317	1.76	0.247	2.87	0.465	0.954	0.497	0.125
KOO-29	26.5	3.10	440	26.2	161	9.08	75.1	10.9	26.8	4.30	20.8	5.62	1.88	0.887	4.89	0.926	2.34	0.341	1.89	0.269	3.78	0.610	1.19	0.679	0.141
KOO-30	25.2	3.13	438	23.5	152	10.3	73.9	16.3	39.6	5.46	23.4	5.42	1.73	0.779	4.25	0.814	2.06	0.297	1.65	0.232	3.67	0.667	1.91	0.881	0.164
KOO-31	-	2.99	409	24.0	152	8.80	71.0	10.7	27.8	4.10	19.7	5.25	1.75	0.815	4.50	0.855	2.14	0.309	1.74	0.243	3.55	0.577	0.951	0.543	0.133
KOO-48	25.5	4.81	435	27.0	142	9.86	103	11.9	30.4	4.62	21.5	5.54	1.85	0.872	4.85	0.923	2.39	0.348	1.90	0.268	3.63	0.658	1.21	0.673	0.168
KOO-50	26.1	0.20	398	29.3	144	9.44	78.4	12.2	27.3	4.44	20.9	5.48	1.87	0.901	5.03	0.993	2.56	0.370	2.02	0.283	3.45	0.607	1.15	0.660	0.123

(1)For sample locations see Frey et al. (1994)

where the lower ratios of the Kalihi-stage lavas overlap with the Mauna Loa field. These differences are not a function of MgO content (Fig. 4b). In detail, however, Units 4, 5 and 6 of the KSDP core overlap with Makapuu-stage lavas in Sr/Nb and Units 4, 6, 14, 73 and 81 overlap in La/Nb (Fig. 3). We use these ratios to address the question—was the transition abrupt or gradual? As shown in Fig. 3, within the uppermost 32 m of the KSDP core, classed as Kalihi-stage by Haskins and Garcia (2004), there are six flows (Units 4, 5, 6, 9, 10 and 12) with geochemical characteristics that are transitional between Makapuu-stage and Kalihi-stage groups. Also, La/Nb and Sr/Nb generally increase upwards from an elevation of ~470 m below sea level, but there are high frequency variations superimposed on these general trends. Within the KSDP core there is no indication that there was an abrupt change from only Kalihi-stage composition to the distinctive Makapuu-stage composition. Rather the Makapuu-stage geochemical signature gradually appears towards the top of the core and is most evident in two groups, Units 4, 5, 6, and Units 9, 10, 12. This inference of a gradual transition from Kalihi-stage to Makapuu-stage geochemical characteristics contrasts with that of Shinozaki et al. (2002), Takahashi and Nakajima (2002) and Tanaka et al. (2002) who described the transition from Mauna Loa-like composition (Kalihi-stage) to Makapuu-stage composition as ''very sharp and abrupt'' occurring over an interval of ~10 m in subaerial outcrops on the Nuuanu Pali.

Haskins and Garcia (2004) argue that the transition from Kalihi- to Makapuu-stage compositions occurred over a 60-m-thick sequence of lavas; consequently, this transition lasted over 2.6–4.6 ka assuming a lava accumulation rate of 13–23 mm per year (DePaolo and Stolper 1996). This estimate may be a minimum because these accumulation rates may be too high for late shield growth (cf. 8.6 to 0.9 mm per year for Mauna Kea, Sharp and Renn (2005). Moreover, we infer that the transition from typical Kalihi-stage composition to Makapuu-stage composition began at the elevation of ~470 m below sea level in the KSDP drill hole, and continued to the top of the cored section at ~300 m below sea level (Fig. 3). This transition corresponds to at least ~60 lava flows (Table 1). If the time interval between flows at a given location is ~1,400 years (estimated from the Mauna Kea portion of the Phase 2 of the Hawaii Scientific Drilling Project core which consists of ~300 shield and late-shield lava flow units erupted over ~410 ka, Sharp and Renne (2005), the transition in composition from Kalihi-stage lavas to Makapuu-stage lavas lasted for ~84 ka which corresponds to a growth rate of ~2 mm per year, and is much longer than the estimate, 2.6–4.6 ka, of Haskins and Garcia (2004). Consequently, in agreement with Haskins and Garcia (2004) we conclude that the transition was not caused by a catastrophic event, such as the Nuuanu landslide.

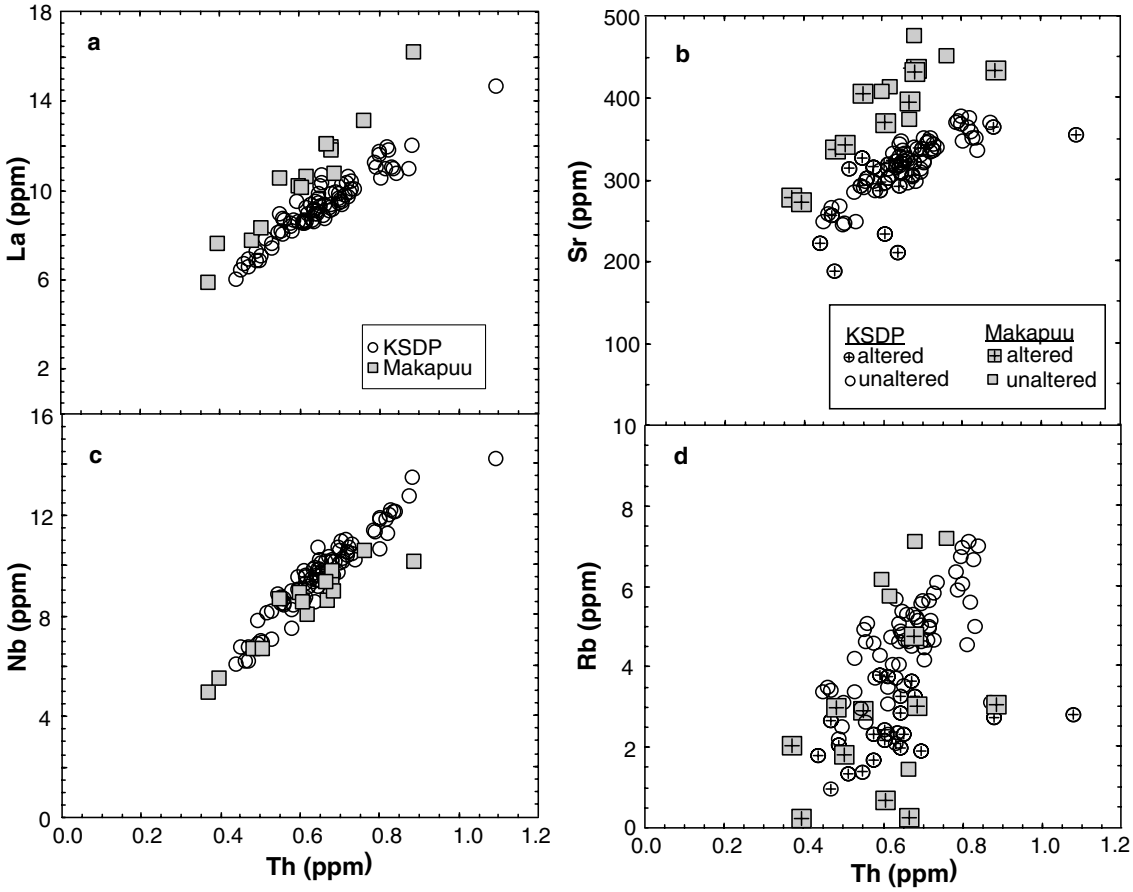

Fig. 1 Th abundance versus other incompatible element abundances. The greater scatter of Rb and Sr reflects post-magmatic alteration; unaltered lavas are lavas with $2.2 > K_2O/P_2O_5 > 1.2$ and Loss on Ignition (L.O.I.) $< 0.8\%$ (Haskins and Garcia, 2004). Data from Tables 1 and 2

Role of recycled marine sediment in the source of Koolau lavas

What is the source of the distinctive Makapuu-stage geochemical signatures? Several characteristics of Makapuu-stage lavas, such as high La/Nb, high $^{176}Hf/^{177}Hf$ at a given $^{143}Nd/^{144}Nd$ and relatively high $^{187}Os/^{188}Os$ and $\delta^{18}O$, have been proposed as recycled sediment signatures (Lassiter and Hauri 1998; Jackson et al. 1999; Blichert-Toft et al. 1999; Huang and Frey 2003). In the KSDP core, depth profiles of $^{208}Pb^*/^{206}Pb^*$, $^{143}Nd/^{144}Nd$ and $^{176}Hf/^{177}Hf$ (Fekiacova et al., in preparation; Salters et al. in preparation) are similar to those of La/Nb and Sr/Nb. Consequently, Makapuu-stage and Kalihi-stage lavas form trends in La/Nb versus $^{208}Pb^*/^{206}Pb^*$ and $^{143}Nd/^{144}Nd$ plots (Fig. 5a, c). Clearly, these lavas were derived from a source containing two geochemically-distinct components. One component is like Mauna Loa lavas (Figs. 5a, c), but the other component defines an endmember with high $^{208}Pb^*/^{206}Pb^*$ (Fig. 5c, d). Since marine sediments typically have higher ^{232} Th/^{238} U and lower ^{238} U/^{204}Pb than primitive mantle values (e.g., Figs. 11 and 12 of Ben Othman et al. 1989), ancient recycled sediments are characterized by relatively low $^{206}Pb/^{204}Pb$ and high $^{208}Pb/^{204}Pb$ at a given $^{206}Pb/^{204}Pb$, i.e., high $^{208}Pb^*/^{206}Pb^*$. Therefore, Pb isotopic ratios of Makapuu-stage lavas are also consistent with ancient recycled marine sediment in their source.

The correlations in Figs. 4 and 5 require that the inferred sedimentary component has high La/Nb (> 1.6), Sr/Nb (> 55) and low Th/La (< 0.05). We note that, based on corrections of La, Sr and Nb with Th (Fig. 1), the high La/Nb and Sr/Nb in Makapuu-stage Koolau lavas (Fig. 4) reflect relative enrichment of La and Sr rather than depletion of Nb. We ask—Are these characteristics of marine sediment? Sr/Nb and Th/La are highly variable in marine sediments (Fig. 6; Fig. 2 of Plank 2005); however, most carbonate- and phosphate-rich ($CaO > 20\%$, $Al_2O_3/P_2O_5 < 10$) sediments are characterized by high Sr/Nb (> 55) and low Th/La (< 0.05) (Fig. 6). In addition, the hydrothermal clay section recovered from east of the Tonga trench, which is also phosphate-rich, has these geochemical characteristics (Fig. 6; Table 1 of Plank and Langmuir 1998). Only small amounts of phosphate-bearing carbonate (3%) or hydrothermal clay (0.25%) are required to explain the high La/Nb and low Th/La that are characteristic of Makapuu-stage lavas (see source compositions in Table 3). High Sr/Nb (> 55) is also consistent with 3% phosphate-bearing carbonate

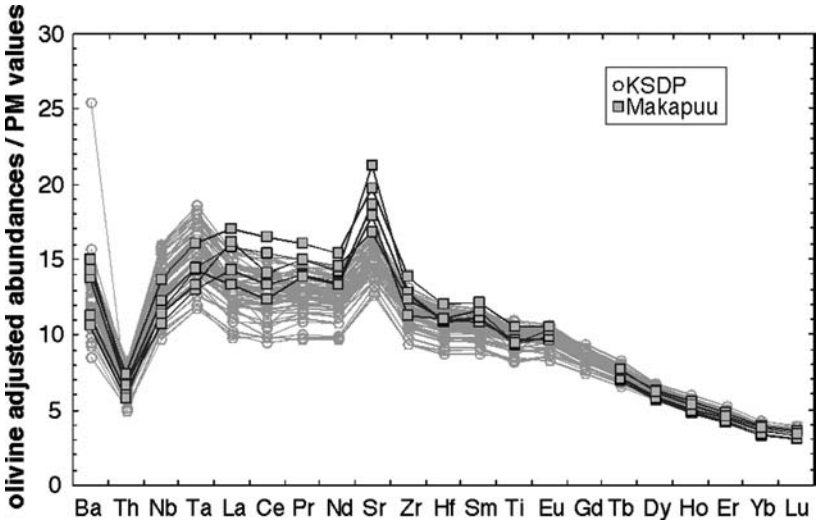

Fig. 2 Primitive mantle normalized trace element abundances in Makapuu-stage and Kahili-stage lavas. Primitive mantle values are from Hofmann (1988). Measured incompatible element abundances in unaltered lavas with $2.2 > K_2O/P_2O_5 > 1.2$ and MgO > 6.5% were adjusted by adding or subtracting equilibrium olivine until the whole rock Fe/Mg ratio was in equilibrium with Fo_{90} olivine (0.1% increments using $(Fe/Mg)_{olivine}/(Fe/Mg)_{melt} = 0.30$). Data from Table 1

but is inconsistent with only 0.25% hydrothermal clay, similar to that recovered from east of the Tonga trench (see source compositions in Table 3). However, given the variable Sr content of hydrothermal sediments (e.g., Thompson et al. 1988; Honnorez et al. 1999), we do not preclude hydrothermal sediment as a possible component in the source of Makapuu-stage lavas.

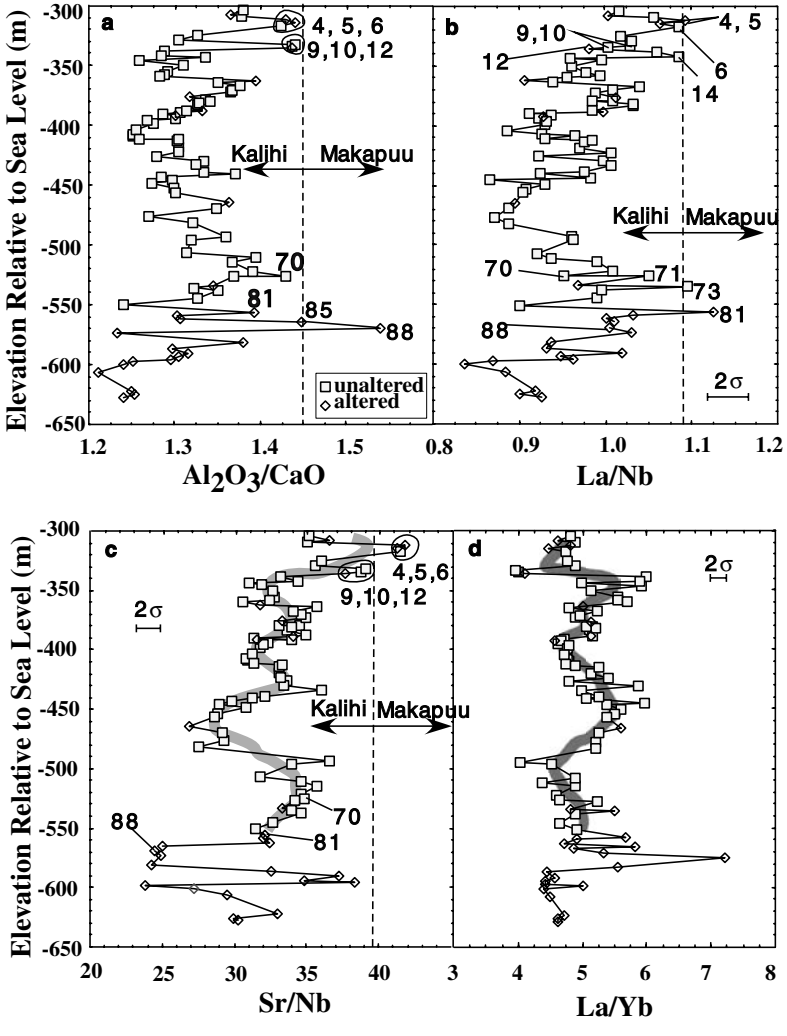

Fig. 3 Depth profiles of Al_2O_3/CaO, La/Nb, Sr/Nb and La/Yb for KSDP drill hole. (2σ analytical uncertainties for La/Nb, Sr/Nb and La/Yb are from Appendix of Huang and Frey (2003), and 2σ analytical uncertainty for Al_2O_3/CaO is less than the symbol size (Rhodes, 1996)). All lavas from the KSDP core were classified as Kalihi-stage lavas by Haskins and Garcia (2004). The Makapuu/Kalihi-stage compositional boundary, vertical dashed lines, is taken as $Al_2O_3/CaO = 1.45$ (Haskins and Garcia, 2004), La/Nb = 1.09 and Sr/Nb = 39.4 (lowest values in Makapuu-stage lavas; Fig. 4). There is considerable structure in these depth profiles. Al_2O_3/CaO, La/Nb and Sr/Nb generally increase upwards from an elevation of ~470 m below sea level, but there are superimposed high frequency variations. The depth profiles of Sr/Nb and La/Yb are highlighted by thick gray lines (defined by running means for every five samples). The former contains several cycles and a secular trend of increasing Sr/Nb with decreasing depth. The latter contains several cycles, but lacks a secular trend

Phosphate-bearing carbonate-rich sediments with high Sr/Nb and low Th/La are a regional feature of the equatorial eastern Pacific Ocean; e.g., they occur in the Guatemala trench and basin, as well as in the Peru and Columbia trenches (Plank and Langmuir 1998; Patino et al. 2000; Plank et al. 2002). However, these phosphate-bearing carbonate-rich sediments are associated with biological activity, such as nannofossil and foram deposits that did not exist at 2 Ga. Nevertheless, the high rare earth element content of Proterozoic marine carbonate sediments, such as phosphorites and carbonates associated with banded iron formations, indicate that these sediments are likely to have low Th/La accompanied by high Sr/Nb (e.g., Tu et al. 1985).

Because of their enrichment in rare earth elements, such sediments have elevated Lu/Hf. If we use data for modern sediments, the carbonate section from Guatemala trench has Lu/Hf = 1.4 and the hydrothermal clay section from east of the Tonga trench has Lu/Hf = 0.47 (Table 1 of Plank and Langmuir 1998); in contrast, the primitive mantle value is 0.24 (Hofmann 1988). Consequently, ancient recycled phosphate-bearing carbonate and hydrothermal sediments are characterized by high $^{176}Hf/^{177}Hf$ at a given $^{143}Nd/^{144}Nd$, which is consistent with the shallow slope of the Hawaiian shield lava trend in an ε_{Nd}–ε_{Hf} plot (Fig. 2 of Blichert-Toft et al. 1999).

The inferred sedimentary component in Koolau lavas must have high $^{87}Sr/^{86}Sr$ (~0.7045, Fig. 14 of Huang and Frey 2003). Hydrothermal sediments are characterized by high Rb/Sr. For example, the hydrothermal clay section from east of the Tonga trench has Rb/Sr = 0.09 (Table 1 of Plank and Langmuir 1998), and the primitive mantle value is 0.03 (Hofmann 1988). Consequently, aged recycled hydrothermal sediments will have relatively high $^{87}Sr/^{86}Sr$. In contrast, phosphate-bearing carbonate-rich sediments are characterized by low Rb/Sr. For example, the carbonate section from the Guatemala trench has Rb/Sr = 0.005 (Table 1 of Plank and Langmuir 1998). Can ancient recycled phosphate-bearing carbonate-rich sediments have relatively high $^{87}Sr/^{86}Sr$? At 2 Ga, seawater $^{87}Sr/^{86}Sr$ was > 0.704 (Fig. 3 of Ray et al. 2002). Consequently, ancient recycled phosphate-bearing carbonate-rich sediments, which inherited $^{87}Sr/^{86}Sr$ from seawater, can explain the high $^{87}Sr/^{86}Sr$ in Makapuu-stage lavas.

Additional evidence supporting marine sediments as a source component for Makapuu-stage lavas arises from correlations between Ce/Pb and La/Nb, Th/La and Ba/Th in Koolau glasses that extrapolate toward a component with low Ce/Pb and Th/La and high Ba/Th and La/Nb (Fig. 7). Compared with MORB and OIB, marine sediments are generally characterized by low Ce/Pb (e.g., Hofmann 1997). Specifically, the carbonate section at Guatemala and the hydrothermal clay section from Tonga have Ce/Pb = 0.6–0.8 (Table 1 of Plank and Langmuir 1998; Table 2 of Patino et al. 2000). In addition, these sediments have high Ba/Th (>1,000), low Th/La (0.02–0.03) and high La/Nb (18–56). In contrast to the glass data, whole rock data (even after applying an alteration filter) do not form obvious trends in Fig. 7, implying that Ce/Pb and Ba/Th were affected by post-magmatic alteration even in these relatively less altered whole rocks. Nevertheless, the linear trends formed by glass data in Fig. 7 imply a source component with low Th/La, Ce/Pb and high La/Nb and Ba/Th, which is consistent with phosphate-bearing carbonate-rich or hydrothermal sediments as a source component for Koolau lavas.

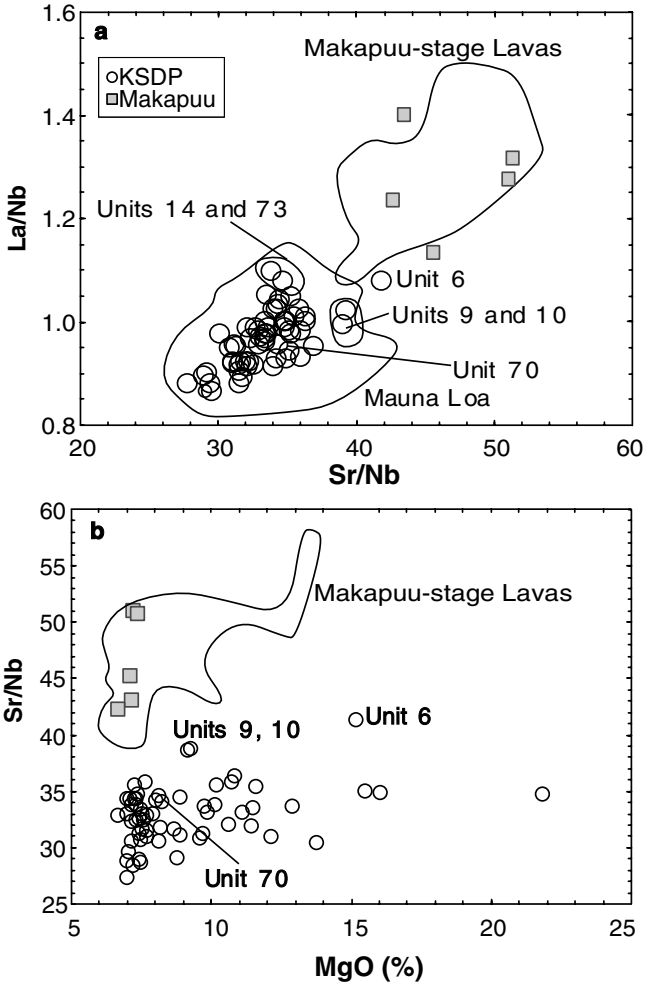

Fig. 4 Sr/Nb vs La/Nb, and MgO (%) versus Sr/Nb for Makapuu- and Kalihi-stage lavas. Only relatively unaltered lavas (Kalihi-stage, Makapuu-stage and Mauna Loa lavas) with $2.2 > K_2O/P_2O_5 > 1.2$ and L.O.I. < 0.8% are plotted. Symbols indicate trace element data from Table 1. Major element data are from Frey et al. (1994) (Makapuu) and Haskins and Garcia (2004) (KSDP), respectively. Fields labeled as "Makapuu-stage Lavas" are defined by XRF and INAA data from Frey et al. (1994). Mauna Loa data are from Garcia et al. (1995a), Rhodes (1995, 1996), Rhodes and Hart (1995), Cohen et al. (1996) and Rhodes and Vollinger (2004), our unpublished trace element data for the Mauna Loa section of HSDP 2

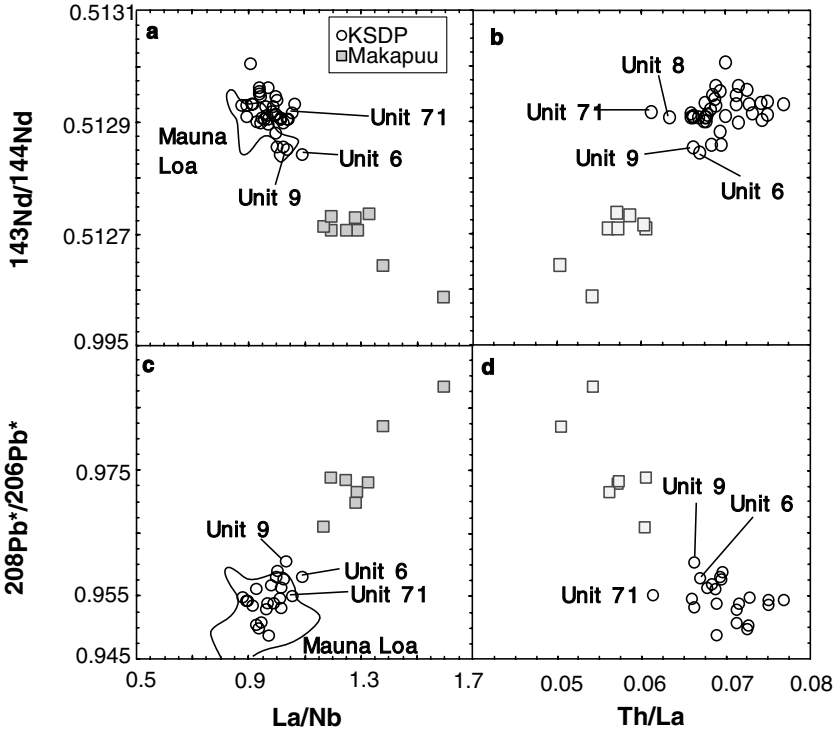

Fig. 5 La/Nb and Th/La versus $^{143}Nd/^{144}Nd$ and $^{208}Pb^*/^{206}Pb^*$ for Makapuu- and Kalihi-stage lavas. $^{208}Pb^*/^{206}Pb^*$ represents the time-integrated $^{232}Th/^{238}U$ since the Earth formation, and is defined as $[(^{208}Pb/^{204}Pb)_{sample}-29.475]/[(^{206}Pb/^{204}Pb)_{sample}-9.307]$ (Galer and O'Nions, 1985). Kalihi-stage lavas overlap with the field defined by Mauna Loa lavas in panels **a** and **c**. The linear trends in these panels imply that the transition from Kalihi-stage composition to Makapuu-stage composition reflects an increasing role of a component with high La/Nb and $^{208}Pb^*/^{206}Pb^*$ coupled with low $^{143}Nd/^{144}Nd$ and Th/La. Since $^{176}Hf/^{177}Hf$ is positively correlated with $^{143}Nd/^{144}Nd$ (Salters et al., in preparation.), the distinctive component in Makapuu-stage lavas also has relatively low $^{176}Hf/^{177}Hf$. Isotopic data for Kalihi-stage lavas are from Salters et al. (in preparation.) and Fekiacova et al. (in preparation.). Isotopic data for Makapuu-stage lavas are from Roden et al. (1994) and Lassiter and Hauri (1998). Mauna Loa data are from Rhodes (1995, 1996), Rhodes and Hart (1995), Cohen et al. (1996), Blichert-Toft et al. (2003) and our unpublished trace element data for the Mauna Loa section of HSDP 2

Relative role of garnet pyroxenite/eclogite and peridotite as sources for Koolau lavas: trace element constraints

After Koolau whole rock compositions are adjusted to be in equilibrium with a common mantle olivine composition (Fo_{90}), the abundance of heavy rare earth elements is much less variable than those of highly incompatible elements (Fig. 2). This result reflects garnet as a residual mineral during partial melting (Hofmann et al. 1984). Compared with other Hawaiian shield lavas, Makapuu-stage lavas at a given MgO content have lower Sc, Y and Yb abundances, a result interpreted to reflect a larger proportion of residual garnet during generation of Makapuu-stage lavas (Budahn and Schmitt 1985; Frey et al. 1994; Jackson et al. 1999). This observation is confirmed by our ICP-MS data of Makapuu-stage lavas (Fig. 8a, b). Kalihi-stage lavas have higher Sc and Yb abundances than Makapuu-stage lavas, and overlap with (Sc) or are on the lower part of (Yb) the fields defined by Mauna Kea and Mauna Loa lavas (Fig. 8a, b).

The variable presence of a sedimentary component in Koolau lavas indicates that garnet pyroxenite, formed from recycled basaltic oceanic crust, may also be a source component. In subsequent discussion, we use garnet pyroxenite as a general rock name that includes eclogite. Hauri (1996) concluded that Makapuu-stage lavas contain a dacitic component derived from partial melting of quartz-bearing garnet pyroxenite formed from recycled oceanic crust. More recently, Takahashi and Nakajima (2002) inferred that Makapuu-stage lavas were derived from eclogite formed from recycled Fe-rich Archean basalt, whereas Garcia (2002) argued that picritic submarine lavas from the slope of Koolau Volcano were primarily derived from partial melting of peridotite. Hence, the source of Koolau lavas may have been peridotite with embedded garnet pyroxenite heterogeneities. How does melting of such a mixed source proceed? Since the solidi of most garnet pyroxenites are lower than those of peridotite (e.g., Hirschmann and Stolper 1996), one modeling approach is to fertilize the unmelted peridotite with partial melt of garnet pyroxenite to form a homogeneous modified garnet peridotite source. This process is consistent with the experiments by Yaxley and Green (1998) and was used by Sobolev et al. (2000) to model the origin of melt inclusions in olivine in Mauna Loa lavas.

Koolau data consistent with variable partial melting of a garnet peridotite source are the correlated variations in ratios that are controlled by residual garnet, such as

Table 3 Input Parameters for Peridotite Melting Model

	Mineral Proportions			
	Olivine	orthopyroxene	Clinopyroxene	garnet
Source Mode[a]	0.53	0.04	0.38	0.05
Melting Reaction[a]	0.05	−0.49	1.31	0.13
	Partition Coefficients			
	Olivine[b]	orthopyroxene[c]	Clinopyroxene[d]	Garnet[d]
La	0	0.002	0.008[e]	0.023[e]
Zr	0	0.017	0.027	0.411
Hf	0	0.036	0.049	0.517
Tb[f]	0	0.046	0.119	1.72
Yb	0	0.092	0.174	5.17
Y	0	0.060	0.165	2.37
Sc	0.14[g]	0.27[g]	1.4[h]	5.17[i]

Source compositions (abundance in ppm)

	Original source[j]	Guatemala Carbonate Section[k]	Adding 3% carbonate-rich sediment into original source	Tonga Hydrothermal Clay[k]	Adding 0.25% hydrothermal sediment into original source
La	0.67	14	1.1	134	1.0
Nb	0.71	0.79	0.71	2.4	0.71
Zr	10	5.9	10	161	10
Tb	0.085	0.47 [1]	0.096	4.5[l]	0.096
Yb	0.28	1.6	0.32	14	0.31
Y	3.9	32	4.7	154	4.2
Sc	10.8	4.8	11	13	11
Sr	25	1504	69	822	27
Th	0.047	0.29	0.05	3.6	0.06
Th/La	0.070	0.020	0.050	0.027	0.056
La/Nb	0.95	18	1.5	56	1.4
Sr/Nb	35	1904	98	347	38
La/Yb	2.4	9.1	3.4	9.4	3.2
Zr/Yb	36	3.8	31	11	33
Sc/Y	2.8	0.15	2.3	0.08	2.6
Tb/Yb	0.30	0.29	0.30	0.31	0.30

[a]From Table 2 of Salters (1996)
[b]$D^{olivine/melt}$ is assumed to be zero, except for Sc
[c]Sample TM 295-5 (2.8GPa and 1540 °C) from Salters and Longhi (1999)
[d]Sample TM 694-6 (2.8GPa and 1537 °C) from Salters and Longhi (1999)
[e]$D_{La}^{clinopyroxene/melt} = D_{Nb}^{clinopyroxene/melt}$ and $D_{La}^{garnet/La} = D_{Nb}^{garnet/melt}$ are assumed
[f]$D_{Tb} = (D_{Sm} + D_{Er})/2$
[g]$D_{Sc}^{olivine/melt}$ and $D_{Sc}^{orthopyroxene/melt}$ are calculated using mineral and melt composition of Sample TM 295-5 (2.8GPa and 1540 °C) and Equation 39 of Beattie et al. (1991)
[h]$D_{Sc}^{clinopyroxene/melt}$ ranges from 0.8 to 3.2 (e.g., Hart and Dunn, 1993; Hauri et al., 1994a; Blundy et al. 1998) We use $D_{Sc}^{clinopyroxene/melt} = 1.4$ in our modeling
[i]$D_{Sc}^{garnet/melt} = D_{Yb}^{garnet/melt}$ is assumed (e.g., van Westrenen et al., 1999)
[j]Y abundance is taken as the primitive mantle value, and Y/Yb is assumed equal to the ratio in both Makapuu- and Kalihi-stage lavas (13.6 ± 0.8)Other ratios are chosen to fit the trends, and abundances of La, Nb, Tb, Zr and Sc are calculated based on these ratios and abundances of Y and Yb
[k]From Table 1 of Plank and Langmuir, 1998
[l]Tb abundance is calculated assuming $Tb_{PM} = (Gd_{PM} + Dy_{PM})/2$. Primitive mantle values are from Hofmann (1988)

La/Yb, Sc/Y and Tb/Yb, in Kalihi-stage and Makapuu-stage lavas (Fig. 9). The La/Yb–Sc/Y, La/Yb–Zr/Yb and La/Yb–Tb/Yb trends can be explained by partial melting of a garnet peridotite, with uniform La/Yb, Sc/Y, Zr/Yb and Tb/Yb (Fig. 9). These ratios may have been similar in the sources of Kalihi-stage and Makapuu-stage lavas because adding a small amount (< 3%) of sediment into the proposed source for Kalihi-stage lavas has little effect on these ratios. For example, adding 3% phosphate-bearing carbonate-rich sediment into the proposed source for Kalihi-stage lavas markedly increases La/Nb from 0.95 to 1.5, Sr/Nb from 35 to 98 and decreases Th/La from 0.07 to 0.05, but only changes La/Yb by < 50%, and Sc/Y, Zr/Yb and Tb/Yb by < 15% (Table 3). In contrast, La/Yb, Sc/Y, Zr/Yb and Tb/Yb in Makapuu-stage and Kalihi-stage lavas vary by a factor of > 2, ~1.7, > 2 and ~1.2, respectively (Fig. 9). We infer that Makapuu-stage lavas were derived by lower extents of melting than Kalihi-stage lavas. Consequently, they equilibrated with a larger amount of residual garnet.

Although we are confident that abundance ratios sensitive to control by residual garnet were controlled by the melting process, the simple model of variable extents of partial melting of garnet peridotite is not suitable. Eggins (1992) and Wagner and Grove (1998) showed that the estimated primary magma compositions for

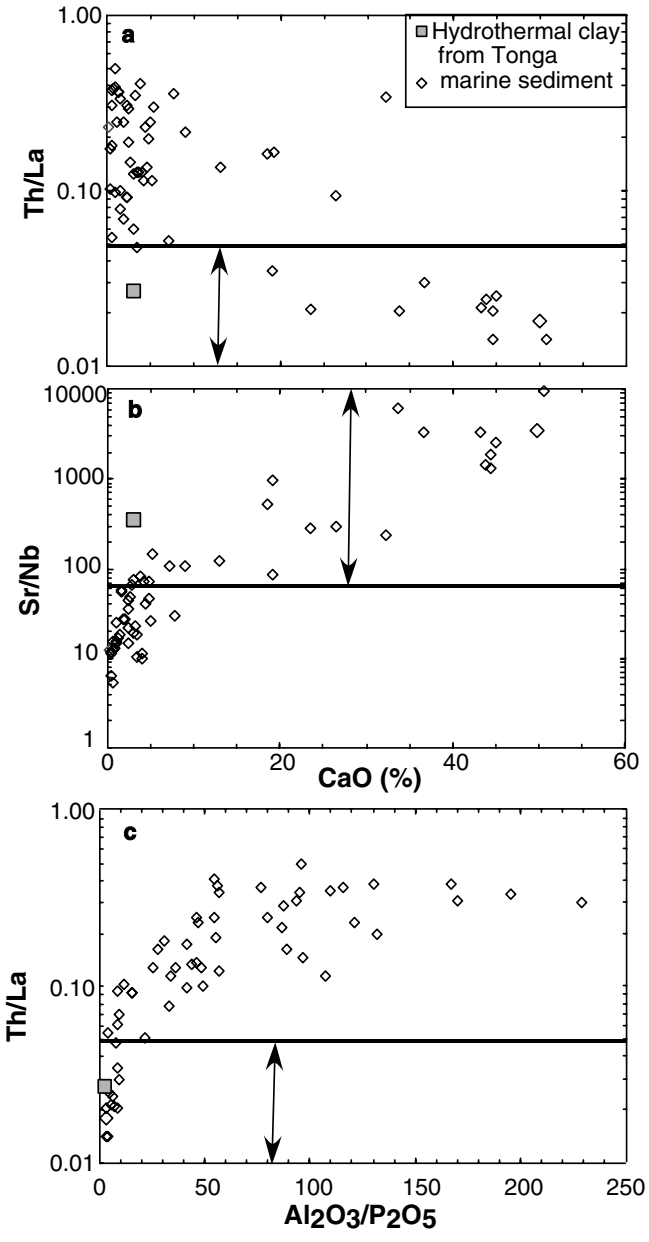

Fig. 6 CaO versus Th/La and Sr/Nb, and Al_2O_3/P_2O_5 versus Th/La for different marine sediment sections. Arrows show sediments with Th/La < 0.05 and Sr/Nb > 55, similar to extreme Makapuu-stage ratios (Figs. 4, 5). Such sediments are CaO- and P_2O_5-rich sediments or hydrothermally-derived clays, such as those from the Tonga trench. Data are from Plank and Langmuir (1998), Patino et al. (2000) and Plank et al. (2002)

Hawaiian shield lavas, and especially, Makapuu-stage lavas (Hauri 1996), are not in equilibrium with garnet peridotite. More complex models are required.

One possibility is mixing of melts derived from garnet peridotite and garnet pyroxenite. However, La/Yb is not correlated with Sr–Nd–Pb isotopic ratios; therefore, the trends formed by Koolau lavas in Fig. 9 are not magma mixing trends. Rather we infer that Koolau lavas reflect both variable extents of partial melting and magma mixing processes. That is, the transition from Kalihi-stage to Makapuu-stage was accompanied by decreasing melting extent and an increasing proportion of a garnet pyroxenite melt component. In this scenario, a complexity is that melts of garnet pyroxenite are very reactive with peridotite and require transport in isolated channels (e.g., Yaxley and Green 1998; Takahashi and Nakajima 2002; Kogiso et al. 2004). That is, the SiO_2-rich melts derived by partial melting of garnet pyroxenite react with peridotite and convert olivine to orthopyroxene (e.g., Yaxley and Green 1998; Takahashi and Nakajima 2002). It is possible that the orthopyroxene band formed between SiO_2-rich melt and peridotite precludes further reaction. Consequently, there is a possibility that SiO_2-rich melts ascend to a magma chamber or even to the Earth's surface. The presence of adakite, which is proposed as partial melt of subducting oceanic crust (e.g., Yogodzinski et al. 1995), provides evidence for this possibility. A requirement of this hypothesis is that the garnet pyroxenite body should be large in size, probably several kilometers, in order to generate sufficient SiO_2-rich melt to form isolated channels insulated from reaction by orthopyroxene bands (Takahashi and Nakajima 2002). Since melt derived from garnet pyroxenite has been proposed to be a significant (Hauri 1996) or even dominant component (Takahashi and Nakajima 2002) for the Makapuu-stage of Koolau, we ask: is it possible to use trace element abundances to distinguish between garnet pyroxenite and garnet peridotite as sources for Makapuu-stage lavas?

Based on experiments in the CMAS (CaO, MgO, Al_2O_3 and SiO_2) system, van Westrenen et al. (2001; see their Fig. 5d) proposed that Zr/Yb can be used to distinguish between melts derived from garnet pyroxenite and garnet peridotite. This discriminant arises because $D_{Zr}^{garnet/melt} > 1$ for the Ca-rich garnet in garnet pyroxenite, and consequently D_{Zr} is similar to D_{Yb}, but $D_{Zr}^{garnet/melt} < D_{Yb}^{garnet/melt}$ for the Mg-rich garnet in garnet peridotite. However, recent experimental results for more complex compositional systems, notably including Ti, show that Zr is not compatible in Ca-rich garnet (Pertermann et al. 2004). Rather than Zr/Yb, Pertermann et al. (2004) propose Zr/Hf as a discriminant for distinguishing residual eclogite (high clinopyroxene/garnet ratio) from residual garnet peridotite (low clinopyroxene/garnet ratio). The suitability of Zr/Hf as a discriminant arises because: (1) $(K_D)_{Zr/Hf}$ for clinopyroxene/melt is ~0.5 whereas it is ~1 for garnet/melt; (2) the very different clinopyroxene/garnet ratios for eclogite and garnet peridotite used by Pertermann et al. (2004). However, clinopyroxene/garnet ratios in peridotite are very dependent upon pressure and temperature (e.g., Walter 1998), and may overlap with the ratios in eclogite; therefore, we suggest that Zr/Hf is not a reliable discriminant. Moreover, Fig. 10 of Pertermann et al. (2004) is misleading because as Koolau lavas they include data from both tholeiitic Koolau shield stage lavas and highly alkalic rejuvenated stage lavas erupted onto the Koolau shield (i.e., the Honolulu Volcanics).

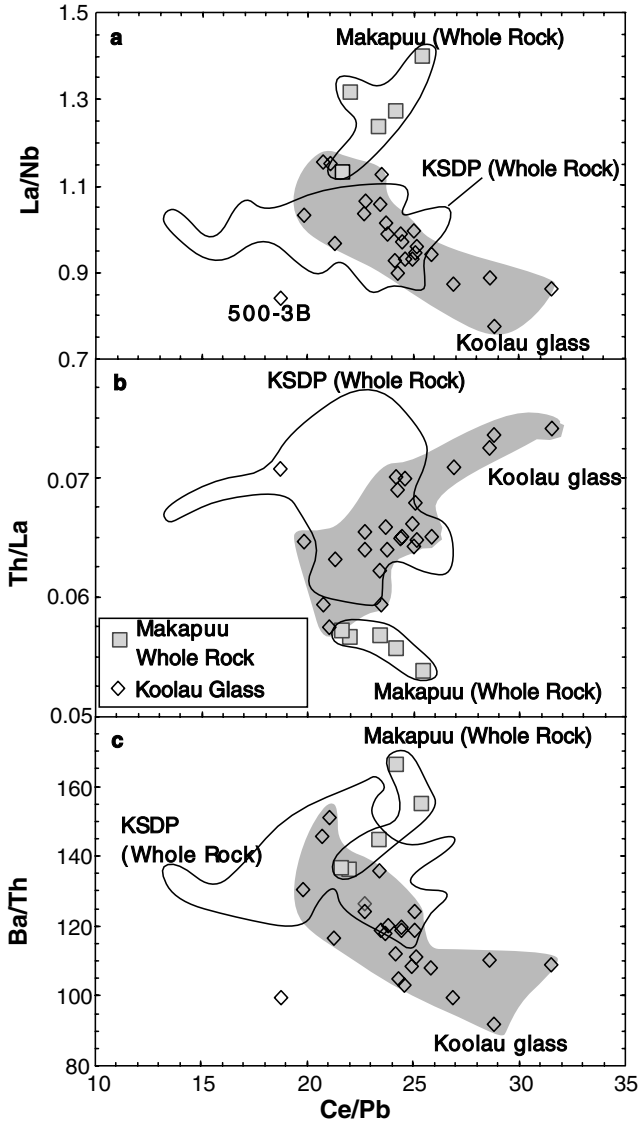

Fig. 7 Ce/Pb versus La/Nb, Th/La and Ba/Th for Koolau glasses (*shaded field*), as well as relatively unaltered whole rocks (with $2.2 > K_2O/P_2O_5 > 1.2$ and L.O.I. < 0.8%). Except for Sample 500–3B from Norman et al. (2004), Koolau glasses form trends in these panels, requiring a component with low Ce/Pb, Th/La and high La/Nb, Ba/Th. Glass data are from Haskins and Garcia (2004) and Norman et al. (2004)

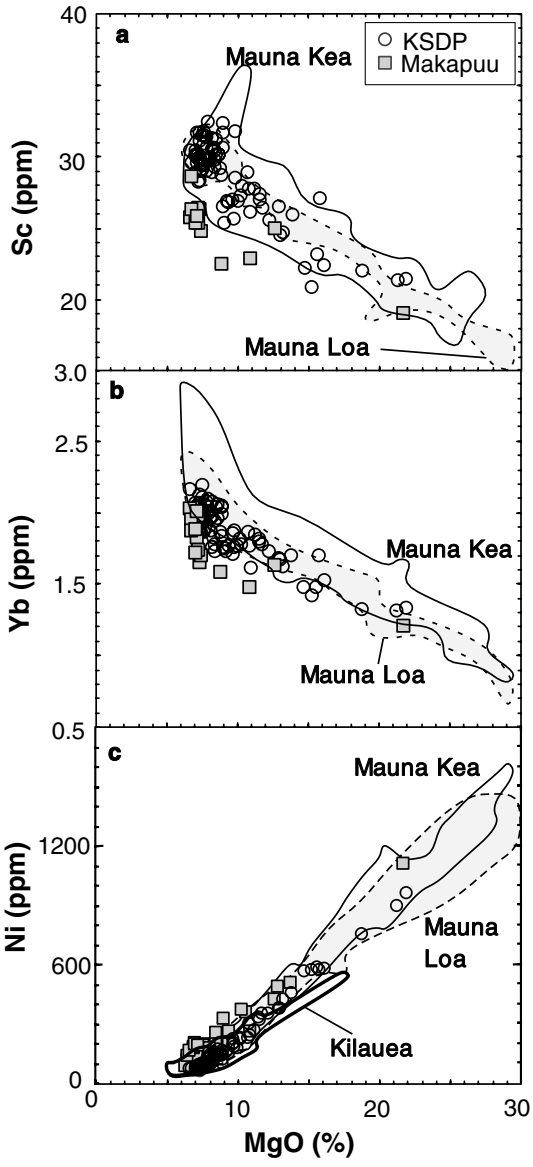

Fig. 8 MgO versus Sc, Yb and Ni for Makapuu-stage and Kalihi-stage lavas. Fields for Mauna Kea, Mauna Loa and Kilauea lavas shown for comparison. Relative to Kalihi-stage, Mauna Loa, Mauna Kea and Kilauea lavas, Makapuu-stage lavas have lower Sc and Yb and higher Ni abundances. For Ni also see Garcia (2002) and Fig. 1 of Sobolev et al. (2005). Data sources: Kalihi-stage lavas (MgO–Ni: Haskins and Garcia, 2004; Sc–Yb: this study); Makapuu-stage lavas (MgO–Ni: Frey et al., 1994; Sc–Yb: this study); Mauna Kea: (MgO–Ni: Rhodes, 1996; Rhodes and Vollinger, 2004; Sc–Yb: Huang and Frey 2003); Mauna Loa (Garcia et al. 1995a; Rhodes 1995, 1996; Rhodes and Hart 1995; Cohen et al. 1996; Rhodes and Vollinger 2004); Kilauea (Garcia et al. 2000)

Relative role of garnet pyroxenite/eclogite and peridotite as sources for Koolau lavas: major element constraints

An early hypothesis for explaining the distinctive major element composition of Makapuu-stage lavas, i.e., relatively high SiO_2 and low total iron and CaO contents, was melt segregation at relatively low pressure (Frey et al. 1994; Putirka 1999). However, Hauri (1996) noted problems with this interpretation. Namely the high SiO_2 content of Makapuu-stage lavas requires melt segregation at depths of 30–45 km, less than the thickness of Hawaiian lithosphere (Li et al. 2004). Also at low pressure, the experimental total iron contents are lower than observed (Fig. 2 of Hauri 1996). He proposed an alternative hypothesis that the distinctive Makapuu-stage composition reflects SiO_2-rich partial melts derived from a garnet pyroxenite component in the plume.

Based on melt-peridotite reactions first discussed in Kelemen (1986), a third alternative for generating relatively high SiO_2 content was proposed by Stolper et al. (2004) for the High-SiO_2 Group Mauna Kea lavas recovered in Phase 2 of the Hawaii Scientific Drilling

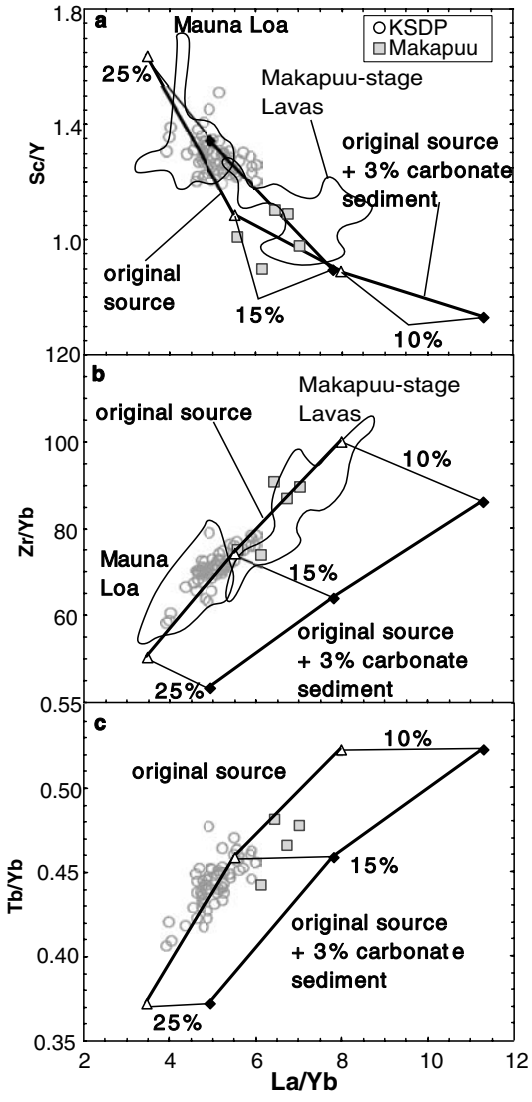

Fig. 9 La/Yb versus Sc/Y, Zr/Yb and Tb/Yb for Makapuu-stage and Kalihi-stage lavas. Fields for Mauna Loa and Makapuu-stage lavas defined by XRF and INAA data are also shown for comparison. Since Tb data obtained by INAA are not very precise (Fig. A5 of Huang and Frey 2003), the fields for Makapuu-stage lavas and Mauna Loa lavas defined by INAA data are not plotted in panel **c**. Only lavas with $2.2 > K_2O/P_2O_5 > 1.2$ and L.O.I. < 0.8% are plotted. As discussed in the text, the source of Makapuu-stage lavas included a recycled sedimentary component. We consider this complexity in modeling. First, we calculate the trends formed by Makapuu-stage and Kalihi-stage lavas using a common garnet peridotite source; i.e., with the same La/Yb, Sc/Y, Zr/Yb and Tb/Yb ratios. These are the melting trajectories labeled as "original source". Input values for the calculation are in Table 3. Then we add 3% carbonate sediment to this "original source" (Table 3). The melting trajectories labeled as "original source + 3% carbonate sediment" are calculated using this sediment enriched source. Less than 3% sediment is sufficient to explain the distinctive features of Makapuu-stage lavas, such as high Sr/Nb, low Th/La and their Nd–Hf isotopic ratios. The effect of adding 0.25% hydrothermal clay to the "original source" is similar to that of adding 3% carbonate sediment (Table 3); consequently, we do not show modeling trends for this case

Project (HSDP). Specifically, melt generated from peridotite (relatively low SiO_2 content) reacts with an overlying residual peridotite by assimilating orthopyroxene, clinopyroxene and crystallizing olivine thereby increasing the SiO_2 content in the melt. This reaction is similar to the models proposed by Eggins (1992) and Wagner and Grove (1998) to explain the high MgO Kilauea glasses. No attempt has yet been made to explain incompatible element abundance and isotopic ratios of HSDP lavas by this process. In addition, since Ni is much more compatible in olivine than other phases, this process will simultaneously increase SiO_2 content and decrease Ni content. Using mineral and melt compositions given in Table 3 of Stolper et al. (2004) and Equation 39 of Beattie et al. (1991), we obtain $D_{Ni}^{olivine/melt} = 6.59$ and $D_{Ni}^{orthopyroxene/melt} = 1.92$. Since $D_{Ni}^{clinopyroxene/orthopyroxene} < 0.5$ (e.g, Table 2 of Seitz et al. 1999), we take $D_{Ni}^{clinopyroxene/melt} = 0.96$ as a maximum estimate. Consequently, the reaction (Fit A) given in Table 3 of Stolper et al. (2004) predicts that Ni content in high-SiO_2 Mauna Kea group lavas should be ~70% of that in low-SiO_2 Mauna Kea group lavas. However, this is not observed in HSDP2 whole rocks (Fig. 5f of Huang and Frey 2003).

With respect to Koolau lavas, the reaction proposed by Stolper et al. (2004) does not significantly affect CaO and Al_2O_3 contents (see their Fig. 18). Therefore, this process does not explain the low CaO and high Al_2O_3/CaO of Makapuu-stage lavas (Fig. 11 of Frey et al. 1994; Fig. 10 of Haskins and Garcia, 2004). In addition, Garcia (2002) noted the unusually high Ni contents of olivine in Koolau lavas and in detail Makapuu-stage lavas have higher Ni contents than Kalihi-stage lavas (Fig. 8c). Consequently, the melt-peridotite reaction fails to explain important compositional features (low CaO and high Ni) of Makapuu-stage lavas. Therefore, this model is not suitable for explaining the SiO_2 difference between Makapuu-stage and Kalihi-stage lavas.

To further evaluate the role of melt derived from garnet pyroxenite in controlling major element compositions of Koolau lavas, the Makapuu-stage and Kalihi-stage lavas, with $K_2O/P_2O_5 > 1.2$ and MgO > 6.5%, were adjusted to be in equilibrium with Fo_{90} olivine, which is the highest Fo olivine found in Makapuu-stage lavas (Norman and Garcia 1999; Garcia 2002), by adding or subtracting equilibrium olivine in 0.1% steps assuming $(Fe/Mg)_{olivine}/(Fe/Mg)_{melt} = 0.30$. After this adjustment, there is still considerable variation in major element composition of Makapuu-stage and Kalihi-stage lavas (Figs. 10, 11). Surprisingly, SiO_2 content does not distinguish Makapuu-stage and Kalihi-stage lavas. Some Kalihi-stage lavas, Units 6 and 9, also have high SiO_2 content (Fig. 10). These two units, along with samples from Units 4, 5, 10 and 12 which are not plotted in Fig. 10, also have the distinctive high Sr/Nb, a characteristic of Makapuu-stage lavas (Fig. 3c). The best major element discriminant between Makapuu-stage

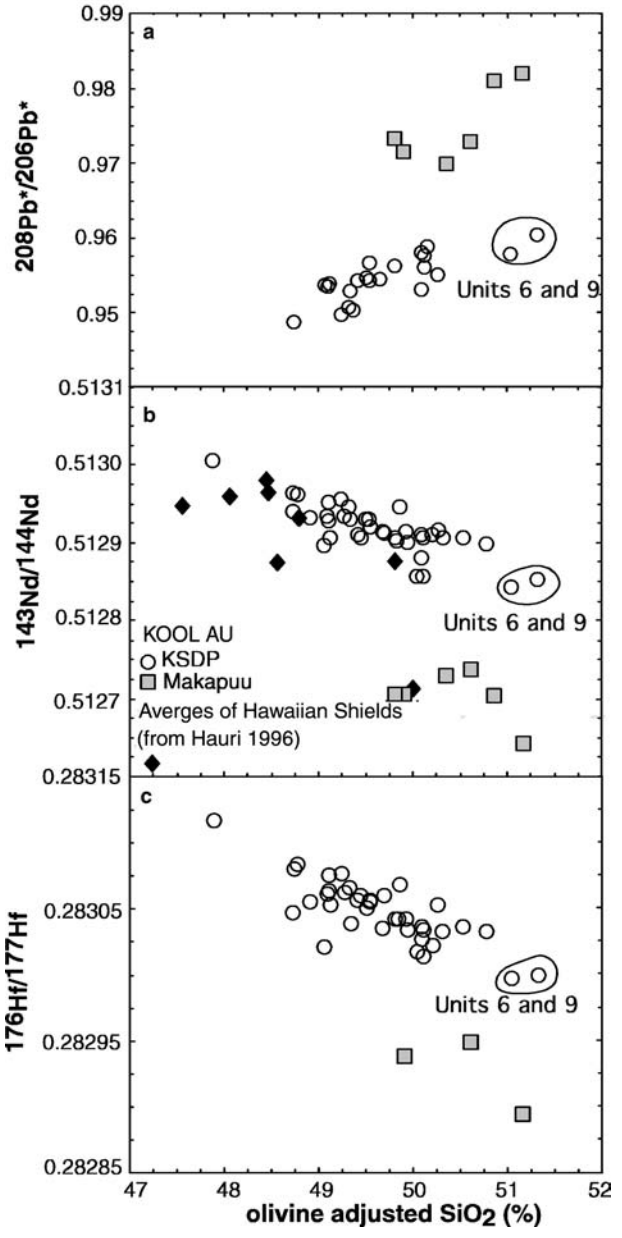

Fig. 10 Olivine adjusted SiO_2 (%) versus $^{208}Pb^*/^{206}Pb^*$, $^{143}Nd/^{144}Nd$ and $^{176}Hf/^{177}Hf$ for Makapuu-stage and Kalihi-stage lavas. These linear trends show that variations in olivine adjusted major element contents are not artifacts of olivine adjustment, but reflect source heterogeneity in major element composition. Surprisingly, Makapuu-stage and Kalihi-stage lavas form subparallel trends in these panels. Averages of stratigraphic sections from different Hawaiian shields (excluding the Loihi alkalic section) from Table 1 of Hauri (1996) are shown in panel **b**. Data source: See captions of Figs. 5 and 8

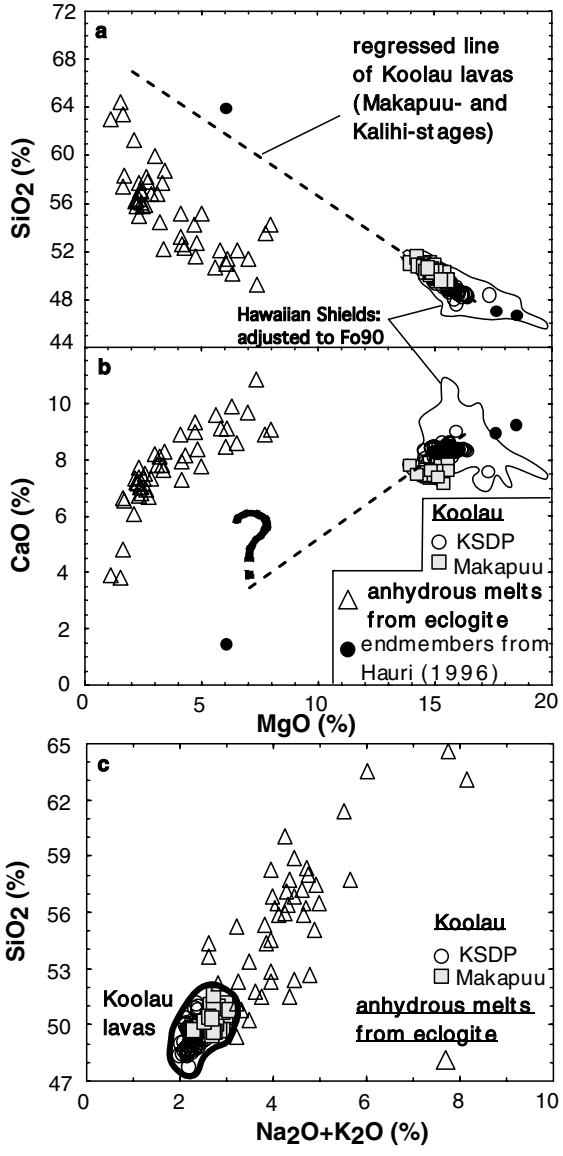

Fig. 11 MgO versus SiO_2 and CaO; and SiO_2 versus $Na_2O + K_2O$. Makapuu-stage (*squares*) and Kalihi-stage (*open circles*) lavas (with $2.2 > K_2O/P_2O_5 > 1.2$ and $MgO > 6.5\%$) are adjusted to be in equilibrium with Fo_{90} olivine. The Hawaiian shield field is defined by olivine adjusted (to be in equilibrium with Fo_{90} olivine) compositions (only lavas with $2.2 > K_2O/P_2O_5 > 1.2$ and $MgO > 6.5\%$ are included). Note that the high SiO_2 component of Hauri (1996) differs from 2–3 GPa partial melts of eclogite (*triangles*, Takahashi et al. 1998; Yaxley and Green 1998; Takahashi and Nakajima 2002; Pertermann and Hirschmann, 2003). Dashed line in Panel **a** is regression trend for Koolau (Makapuu-stage and Kalihi-stage) lavas which intersects the experimental melt trend at $>64\%$ SiO_2; in Panel **b**, the "?" indicates that Koolau lavas do not define a trend. Hawaiian shield data used in this figure are: Koolau (Frey et al. 1994; Haskins and Garcia 2004); Mauna Loa (Garcia et al. 1995a; Rhodes 1995, 1996; Rhodes and Hart 1995; Rhodes and Vollinger 2004); Mauna Kea (Rhodes 1996; Rhodes and Vollinger 2004; Stolper et al. 2004); Kilauea (Chen et al. 1996; Garcia et al. 2000; Quane et al. 2000); Loihi (Frey and Clague 1983; Garcia et al. 1993, 1995b 1998; Norman and Garcia 1999); Kahoolawe (Fodor et al. 1992; Leeman et al. 1994; our unpublished data).

and Kalihi-stage lavas is CaO content (Fig. 11b; Fig. 5 of Haskins and Garcia; 2004). We argued earlier that Makapuu-stage lavas sampled more of a recycled phosphate-bearing carbonate-rich or hydrothermal sedimentary component. Since only small amounts ($< 3\%$) of a sedimentary component is required to explain the

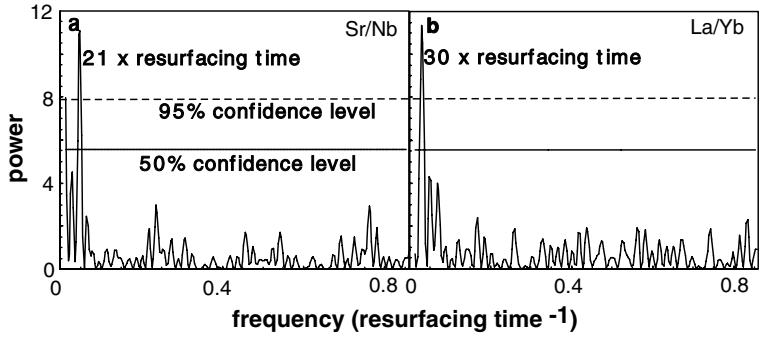

Fig. 12 Lomb normalized periodograms of Sr/Nb and La/Yb for KSDP lavas. Only unaltered lavas ($1.2 < K_2O/P_2O_5 < 2.2$ and L.O.I. < 0.8) are included in the analysis. Two confidence level lines (at 50% and 95%) are shown for comparison. Lomb normalized periodograms of Al_2O_3/CaO, Th/La and La/Nb (not shown) are similar to that of Sr/Nb, i.e., two peaks, and that of Tb/Yb (not shown) is similar to that of La/Yb, i.e., only one peak at ~30 times resurfacing time. The procedure is given by Press et al. (1992, pp 575–579), and Matlab script Lomb.m (http://mathforum.org/epigone/comp.soft-sys.matlab/hangdiher/34CED3BF. B95E25AF@spectral-imaging.com) was used

distinctive trace element geochemical signatures of Makapuu-stage lavas (Table 3), the sedimentary component has negligible effect on the major element content, such as CaO, of Koolau lavas.

Olivine adjusted SiO_2 content in Koolau lavas is correlated with Nd–Hf–Pb isotopic ratios (Fig. 10). Therefore, the large variations in olivine adjusted major element contents are not artifacts of olivine adjustment. In the olivine adjusted SiO_2–$^{143}Nd/^{144}Nd$ plot (Fig. 10b), the averages for different Hawaiian shields (from Table 1 of Hauri 1996) largely overlap with Koolau lavas (Makapuu-stage and Kalihi-stage lavas), implying that a single shield (Koolau) may sample all the source components contributing to Hawaiian shields. Reiners (2002) also noted correlations between composition and isotopic ratios in individual sequences of basaltic eruptives, and he argued for mixing of melts derived from pyroxenite and peridotite. In detail, Makapuu-stage and Kalihi-stage lavas form subparallel trends in Fig. 10. A possible interpretation for these trends is that both Makapuu-stage and Kalihi-stage lavas contain varying proportions of a SiO_2-rich component derived from garnet pyroxenite but that the Makapuu-stage lavas contain more of an isotopically distinctive sedimentary component.

The calculated dacitic magma of Hauri (1996) has an unusual composition in having quite high MgO (6%) for its high SiO_2 content (64%). No experimentally derived melt of eclogite/garnet pyroxenite has these characteristics; in fact, Pertermann and Hirschmann (2003a) concluded that "no eclogitic partial melt has been identified that is capable of explaining all of compositional features of the exotic Koolau component". We ask—Is the 6% MgO–64% SiO_2 a robust estimate? A concern about the Hauri compilation of shield lava composition is SiO_2 mobility during alteration. A significant fraction (26%) of lavas in Hauri's data compilation have $K_2O/P_2O_5 < 1$, and Frey et al. (1994) showed that SiO_2 contents are commonly lower in such altered lavas. However, using our alteration discriminant ($2.2 > K_2O/P_2O_5 > 1.2$) leads to similar averages for Makapuu-stage lavas.

The mismatch between the 6% MgO–64% SiO_2 composition with partial melts of eclogite/garnet pyroxenite is apparent in Fig. 11a. This discrepancy can be avoided by choosing a more SiO_2-rich (~66%) component with ~2% MgO. Although such a dacitic component is consistent with experimentally determined melts of eclogite/garnet pyroxenite, Pertermann and Hirschmann (2003a) suggest that there are two problems with this interpretation:

1.Low degrees of melting of garnet pyroxenite are required to create a SiO_2-rich melt; hence a relatively low temperature is inferred. In contrast, high MgO–low SiO_2 picritic magma requires partial melting of peridotite at higher temperature. Generally, garnet pyroxenite melts to a very high extent (60%) at the peridotite solidus temperature (e.g., Fig. 4 of Pertermann and Hirschmann, 2003b). Consequently, Pertermann and Hirschmann (2003a) suggest that "dacitic partial melts could form from eclogite in the deeper portions or the cold periphery of the plume, with peridotite partial melting predominantly in the hot core"; therefore, they conclude that dacitic and picritic melts are unlikely to be in close proximity. We argue, however, that mixing of such melts is consistent with a physical model for the Hawaiian plume. For example, the radius of the Hawaiian plume is ~50–70 km and the potential temperature in the center of the plume may be ~300–400 °C higher than ambient mantle (Ribe and Christensen 1999; Zhang and Watt 2002). Consequently, there is a large horizontal temperature gradient within the Hawaiian plume (Figs. 4a and 5a of Ribe and Christensen 1999). Since a Hawaiian volcano captures magma generated over a circular area (magma capture area) with radius ranging from 20 to 35 km (DePaolo and Stolper 1996; Ribe and Christensen 1999), the magma capture area can include melts derived over a large temperature range. Using Fig. 4 of Pertermann and Hirschmann (2003b), a temperature difference less than 200 °C is required to generate low extent (10–20%) partial melts of garnet pyroxenite and high extent (~20%) partial

melts of peridotite. Since Makapuu-stage lavas formed as Koolau shield volcanism waned, i.e., when the shield was moving off the plume, the magma capture area included lower temperature dacitic melts.

2.Referring to Norman and Garcia (1999), Pertermann and Hirschmann (2003a) argue that the trace element features created by residual garnet, e.g., high Sr/Y and Sm/Yb, are absent in Koolau lavas. However, in Figs. 2, 8 and 9 we provide evidence for garnet as an important residual phase for Makapuu-stage lavas. Moreover, Fig. 6c of Haskins and Garcia (2004) also shows that a relatively high Sr/Y in Makapuu-stage lavas is consistent with a dacitic component.

Finally, Hawaiian shield lavas define a clear inverse MgO–SiO_2 trend with Makapuu-stage lavas as one extreme (Fig. 11a), but the MgO–CaO plot is scattered (Fig. 11b). Nevertheless, Makapuu-stage lavas are offset to low CaO at a given MgO, and this result is consistent with a low CaO, dacitic component in these lavas (Fig. 11b). Additional evidence in favor of a dacitic component is the positive SiO_2 versus $Na_2O + K_2O$ trend for Koolau lavas (Fig. 11c). This trend can be explained by mixing low SiO_2-low ($Na_2O + K_2O$) picritic melt and high SiO_2-high ($Na_2O + K_2O$) dacitic melt. If the picrite endmember has 48% SiO_2 and 16% MgO, and the dacite endmember has 66% SiO_2 and 2% MgO (Fig. 11a), the maximum amount of dacite endmember in Koolau lavas is ~20%.

Relative role of garnet pyroxenite/eclogite and peridotite as sources for Koolau lavas: Ni constraints

Olivine and whole rocks from Koolau Volcano have unusually high Ni content (Fig. 4 of Garcia, 2002; Fig. 8c). Sobolev et al. (2005) noted that Ni/MgO and SiO_2 (both corrected for olivine fractionation) are positively correlated in Hawaiian shield lavas, with Makapuu-stage lavas defining the high SiO_2 and Ni/MgO endmember. Earlier, we used the relatively high Ni content to argue against a melt–mantle reaction model for explaining high SiO_2. Based on major element contents, we inferred that the high SiO_2 component in Koolau lavas is a dacitic melt; however, dacitic partial melts of eclogites formed from recycled oceanic crust are expected to have low Ni content. In contrast, Sobolev et al. (2005) suggest that high Ni/MgO may be associated with SiO_2-rich melt. They argue that partial melt of garnet pyroxenite reacts with peridotite, replaces olivine with pyroxene, and generates olivine-free, secondary garnet pyroxenite (e.g., Yaxley and Green 1998; Takahashi and Nakajima 2002). Partial melts of this secondary olivine-free, garnet pyroxenite have high Ni and SiO_2 content; therefore, their model accounts for the previously unexplained relatively high Ni and SiO_2 in Makapuu-stage lavas. We note, however, that several aspects of their model need testing. Specifically, can partial melting of olivine-free, secondary garnet pyroxenite generate melts with ~15% MgO and >49% SiO_2 (Table 1 of Sobolev et al. 2005) The high MgO content of this melt is required to keep the bulk-solid/melt partition coefficient for Ni ~1 (Table S2 of Sobolev et al. 2005) rather than >10 for partial melting of MORB-like eclogite (see Table 9 of Pertermann et al. 2004). Finally, a characteristic of Makapuu-stage lavas is relatively low CaO content (Fig. 5 of Haskins and Garcia, 2004 and Fig. 11b, this paper), but low CaO is inconsistent with the relatively high CaO of the calculated melt derived from secondary garnet pyroxenite (Table 1 of Sobolev et al. 2005). Consequently, the model proposed by Sobolev et al. (2005) needs testing and refining before it can be accepted as a suitable model for Makapuu-stage lavas. We agree, however, that mixing of partial melt derived from peridotite and dacitic melt derived from garnet pyroxenite formed from MORB cannot account for anomalously high Ni abundance.

Summary of evidence for ancient recycled oceanic crust in the Hawaiian plume

We have used major and trace element abundances and isotopic data to evaluate garnet pyroxenite as a source component for Koolau lavas. These data show that as Koolau Volcano migrated away from the plume and reached the end of shield building, garnet became increasingly important as a residual phase, the extent of melting decreased and up to 20% of a dacitic melt, with relatively high SiO_2 and low MgO and CaO, contributed to the late shield (Makapuu-stage) lavas. The distinctive trace element and isotopic characteristics of Makapuu-stage lavas, i.e., relatively high La/Nb, Sr/Nb and low Th/La, relatively low $^{143}Nd/^{144}Nd$, but high $^{176}Hf/^{177}Hf$ at a given $^{143}Nd/^{144}Nd$, and relatively high $^{87}Sr/^{86}Sr$ and $^{208}Pb^*/^{206}Pb^*$, can be explained by <3% of a sedimentary component, either ancient recycled phosphate-bearing carbonate or perhaps sediment with an abundant hydrothermal component, in the source. The evidence for a small amount of ancient recycled sediment in the source of late shield Koolau lavas coupled with up to 20% of a dacitic melt derived from garnet pyroxenite are consistent with recycled oceanic crust in the Hawaiian plume. The mixing of high temperature MgO-rich melts required by olivine with $Fo_{88–90}$ (Garcia, 2002) with low temperature dacitic melts is plausible in the Hawaiian plume setting, especially at the end of shield-building, when melts are captured from a region that includes the high temperature plume core and the cooler plume periphery (See Fig. 1 of DePaolo and Stolper 1996).

Temporal geochemical variations within the KSDP core

The relative age of lava flows recovered from the KSDP core is constrained; hence, it is possible to use the time-dependent geochemical variations to constrain temporal

changes in process and the spatial distribution of geochemical heterogeneity. In order to avoid complications caused by alteration, we consider only unaltered lavas ($1.2 < K_2O/P_2O_5 < 2.2$ and L.O.I. < 0.8) in a time series analysis; in particular, we do not consider the bottom of the core where altered lavas are dominant (Fig. 3). We follow the assumption of Blichert-Toft et al. (2003) that the resurfacing time was constant, i.e., the time differences between lava flows were equal. Using the Mauna Kea portion of the Phase 2 of the Hawaii Scientific Drilling Project (HSDP2) core as an analogy for late shield growth of Koolau, we estimate ~1,400 years for resurfacing time (~410 ka for ~300 lava flow units in the Mauna Kea section, Sharp and Renne, 2005). Note that this estimate of resurfacing time exceeds that of 350 years inferred by Blichert-Toft et al. (2003) who erroneously assumed ~1,000 Mauna Kea flow units in the HSDP2 core.

Following the method described in Press et al. (1992, pp 575–579) for time series analysis of an unevenly sampled system, we calculate the Lomb normalized periodograms for Al_2O_3/CaO, Th/La, Sr/Nb, La/Nb, La/Yb and Tb/Yb (Fig. 12). There are two peaks in these periodograms for Al_2O_3/CaO, Th/La, Sr/Nb and La/Nb: one is at very low frequency (unlabeled) and the other is at ~21 times resurfacing time (Fig. 12). These peaks are significant at the 95% confidence level. The low frequency peak reflects the long-term secular trend shown in Fig. 3. In contrast, there is only one peak at ~30 times resurfacing time (significant at 95% confidence level) in the Lomb normalized periodograms for La/Yb and Tb/Yb.

Time series analyses show that the variations of Al_2O_3/CaO, Th/La, Sr/Nb and La/Nb are highly correlated and share a period of ~21 times resurfacing time, which corresponds to ~29 ka using 1,400 years for resurfacing time. The correlations among these ratios are consistent with our inference that high Al_2O_3/CaO arises from partial melting of garnet pyroxenite and the high Sr/Nb, La/Nb with low Th/La arise from an ancient sediment component in this garnet pyroxenite. These variations reflect horizontal (e.g., DePaolo et al. 2001) or vertical (e.g., see Figs. 12 and 13 of Blichert-Toft et al. 2003) geochemical heterogeneity in the Hawaiian plume. Blichert-Toft et al. (2003) note that plume upwelling velocity is greater than plate velocity; therefore magma extraction may homogenize horizontal heterogeneity, thereby, implying that temporal geochemical variations in lavas reflect vertical heterogeneity within the plume. This implication is valid for piston or pipe flow where there is an abrupt velocity gradient between the plume core and rim, but it is less likely if there is a broad velocity gradient (e.g., Hauri et al. 1994b).

If the observed variations of Al_2O_3/CaO, La/Nb, Sr/Nb and Th/La in the KSDP core reflect vertical spacing of a garnet pyroxenite component within the Hawaiian plume, the spacing is 2.9–29 km given 10 cm/year and 1 m/year as the lower and upper limits of the plume upwelling velocity (e.g., Ribe and Christensen 1999). This range encompasses the estimate of Takahashi and Nakajima (2002), based on the volume of Makapuu-stage lavas, that entrained eclogite blocks in the Hawaiian plume "may reach up to 10 km in size or larger". The approach of Eisele et al. (2003) for the HSDP drill core at Mauna Kea calculates the spacing of Pb isotopic heterogeneities by integrating over a non-linear ascent path beneath the HSDP drill site (see their Fig. 13); they infer 21 to 86 km as the minimum length scale of the Pb heterogeneity. However, this approach requires information about the distance between the shield and plume center as a function of time. Such information is not available for Koolau.

The lack of a significant peak (at 95% confidence level) at ~21 times resurfacing time in the Lomb normalized periodograms for La/Yb and Tb/Yb implies that these ratios were not affected by the recycled oceanic crust component. That is, La/Yb and Tb/Yb are controlled by the partial melting process. The variations of La/Yb and Tb/Yb, at a period of ~30 times resurfacing time which corresponds to ~42 ka, imply that there was substantial variation in melting extent during the shield building stage (Figs. 3d, 9). Variable extents of melting during shield construction have also been inferred for Kilauea (Pietruszka and Garcia 1999), Mauna Loa (Rhodes and Hart 1995) and Mauna Kea (Stolper et al. 2004).

Summary

Geochemical and petrographic studies of surface lavas erupted on the Koolau shield and drill core from the KSDP show that the shield lavas changed markedly near the end of shield-building (Frey et al. 1994; Roden et al. 1994; Jackson et al. 1999; Haskins and Garcia 2004; this paper). Specifically, as shield building ended, tholeiitic shield basalt changed gradually from a Mauna Loa-like composition to the well-known geochemical endmember that characterizes subaerially exposed Koolau lavas (i.e., the Kalihi- and Makapuu-stages, respectively of Haskins and Garcia 2004). This transition, occurring over ~84 ka, was not abrupt; therefore, it was not caused by a rapid catastrophic event, such as the Nuuanu landslide. The transition from Kalihi-stage to Makapuu-stage lavas reflects changes in source material that occurred as Koolau volcano migrated away from the plume.

The distinctive geochemical characteristics of Makapuu-stage basalt are manifested in major and trace element abundances as well as isotopic ratios. Relatively low abundances of MgO, CaO, Sc and Yb coupled with high SiO_2 content are consistent with up to 20% of a dacitic melt derived from garnet pyroxenite. Distinctive trace element ratios, such as high La/Nb, Sr/Nb and low Th/La, which correlate with isotopic ratios of Nd, Hf and Pb, provide evidence for $< 3\%$ of ancient recycled (phosphate-bearing carbonate-rich or hydrothermal)

sediment in the source. The combination of kilometer-size garnet pyroxenite and a sedimentary geochemical signature strongly suggests recycled oceanic crust in the Hawaiian plume as Koolau Volcano entered the late-stage of shield construction. Mixing of low temperature dacitic melt formed from garnet pyroxenite and high temperature melt derived from peridotite is possible at this stage of volcano growth, because the magma capture area includes high temperature melts from the plume center and low temperature melts from the cooler periphery of the plume.

Acknowledgements This research was supported by NSF Grant EAR-0105557. Expenses associated with coring were partially supported by funds from the University of Hawaii, California Institute of Technology, University of California at Berkeley, Massachusetts Institute of Technology, Carnegie Institute of Washington, Max-Plank Institut für Chemie, Woods Hole Oceanographic Institute and Tokyo Institute of Technology. We especially thank M. O. Garcia (University of Hawaii) for his origination and leadership of the KSDP. We thank V. J. M. Salters and Z. Fekiacova for sharing their Nd, Hd and Pb isotopic data for the KSDP samples that we studied, B. Grant, R. Kayser and S. Higgins for their assistance in ICP-MS analysis, and F. Dudas for help in the clean lab. We also appreciate the constructive review comments of Terry Plank and an anonymous reviewer, as well as helpful comments from S. W. Parman, V. J. M. Salters, S. A. Bowring and J. P. Grotzinger. We thank Tim Grove for editorial handling. We thank A. V. Sobolev for providing his in press Nature paper.

References

Beattie P, Ford C, Russell D (1991), Partition coefficients for olivine-melt and orthopyroxene-melt system. Contrib Mineral Petrol 109(2):212–224

Ben Othman D, White WM, Patchett J (1989), The geochemistry of marine sediments, island arc magma genesis, and crust-mantle recycling. Earth Planet Sci Letts 94(1–2):1–21

Blichert-Toft J, Frey FA, Albarede F (1999), Hf isotope evidence for pelagic sediments in the source of Hawaiian basalts. Science 285(5429):879–882

Blichert-Toft J, Weis D, Maerschalk C, Agranier A, Albarède F (2003), Hawaiian hot spot dynamics as inferred from the Hf and Pb isotope evolution of Mauna Kea volcano. Geochem Geophys Geosyst 4(2):8704 doi:10.1029/2002GC000340

Blundy JD, Robinson JAC, Wood BJ (1998), Heavy REE are compatible in clinopyroxene on the spinel lherzolite solidus. Earth Planet Sci Lett 160:493–504

Budahn JR, Schmitt RA (1985), Petrogenetic modeling of Hawaiian tholeiitic basalts; a geochemical approach. Geochim Cosmochim Acta 49(1):67–87

Chen C-Y, Frey FA, Rhodes JM, Easton RM (1996), Temporal geochemical evolution of Kilauea Volcano: comparison of Hilina and Puna Basalt. In: Basu A, Hart SR (eds) Earth processes: reading the isotopic code. Geophysical Monograph Series, vol 95. AGU, Washington, pp 161–181

Cohen AS, O'Nions RK, Kurz MD (1996), Chemical and isotopic variations in Mauna Loa tholeiites. Earth Planet Sci Lett 143:111–124

DePaolo DJ, Stolper EM (1996), Models of Hawaiian volcano growth and plume structure; implications of results from the Hawaii Scientific Drilling Project. J Geophys Res 101(5):11,643–11,654

DePaolo D, Bryce J, Dodson A, Shuster D, Kennedy B (2001), Isotopic evolution of Mauna Loa and the chemical structure of the Hawaiian plume. Geochem Geophys Geosyst, 2; doi:10.1029/2000GC000139

Eggins SM (1992), Petrogenesis of Hawaiian tholeiites; 1, Phase equilibria constraints. Contrib Mineral Petrol 110(2–3):387–397

Eisele J, Abouchami W, Galer SJG, Hofmann AW (2003), The 320 kyr Pb isotope evolution of Mauna Kea lavas recorded in the HSDP-2 drill core. Geochem Geophys Geosyst 4(5):8710, doi:10.1029/2002GC000339

Fodor RV, Frey FA, Bauer GR, Clague DA (1992), Ages, rare-earth element enrichment, and petrogenesis of tholeiitic and alkalic basalts from Kahoolawe Island, Hawaii. Contrib Mineral Petrol 110:442–462

Frey FA, Clague DA (1983), Geochemistry of diverse basalt types from Loihi Seamount, Hawaii; petrogenetic implications. Earth Planet Sci Letts 66:337–355

Frey FA, Rhodes JM (1993), Inter-shield geochemical differences among Hawaiian volcanoes: implications for source compositions, melting processes and magma ascent paths. Philos. Trans R Soc Lond A 342:121–136

Frey FA, Garcia MO, Roden MF (1994), Geochemical characteristics of Koolau Volcano: Implications of intershield geochemical differences among Hawaiian volcanoes. Geochim Cosmochim Acta 58:1441–1462

Galer SJG, O'Nions RK (1985), Residence time of thorium, uranium and lead in the mantle with implications for mantle convection. Nature 316(6031):778–782

Garcia MO, Jorgenson BA, Mahoney JJ, Ito E, Irving AJ (1993), An evaluation of temporal geochemical evolution of Loihii summit lavas: Results from Alvin submersible dives J Geophys Res 98:535–550

Garcia MO, Foss DJP, West HB, Mahoney JJ (1995b), Geochemical and isotopic evolution of Loihi Volcano, Hawaii. J Petrol 36:1647–1644

Garcia MO, Hulsebosch TP, Rhodes JM (1995a), Olivine-rich submarine basalts from the southwest rift zone of Mauna Loa Volcano; implications for magmatic processes and geochemical evolution. In: Rhodes JM, Lockwood JP (eds) Mauna Loa Revealed, Geophys Monogr Ser 92:219–239

Garcia MO, Rubin KH, Norman MD, Rhodes JM, Graham DW, Muenow DW, Spencer K (1998), Petrology and geochronology of basalt breccia from the 1996 earthquake swarm of Loihi Seamount, Hawaii; magmatic history of its 1996 eruption. Bull Volcan 59:577–592

Garcia MO, Pietruszka AJ, Rhodes JM, Swanson K (2000), Magmatic processes during the prolonged Pu'u O'o eruption of Kilauea volcano, Hawaii. J Petrol 41(7):967–990

Garcia MO (2002), Giant landslides in the northeast of O'ahu; when, why and how?. In: Takahashi E, Lipman PW, Garcia MO, Naka J, Aramaki S (eds) Hawaiian volcanoes; deep underwater perspectives, Geophys Monogr Ser 128. pp 221–222

Hart SR, Dunn T (1993), Experimental cpx/melt partitioning of 24 trace elements. Contrib Mineral Petrol 113(1):1–8

Haskins ER, Garcia MO (2004), Scientific drilling reveals geochemical heterogeneity within the Ko'olau shield, Hawai'i. Contrib Mineral Petrol 147:162–188

Hauri EH, Wagner TP, Grove TL (1994a), Experimental and natural partitioning of Th, U, Pb and other trace elements between garnet, clinopyroxene and basaltic melts. Chem Geol 117(1–4):149–166

Hauri EH, Whitehead JA, Hart SR (1994b), Fluid dynamic and geochemical aspects of entrainment in mantle plumes. J Geophys Res 99(12):24,275–24,300

Hauri EH (1996) Major-element variability in the Hawaiian mantle plume. Nature 382:415–419

Hirschmann MM, Stolper EM (1996) A possible role for garnet pyroxenite in the origin of the "garnet signature" in MORB. Contrib Mineral Petrol 124(2):185–208

Hofmann AW, Feigenson MD, Raczek I (1984) Case studies on the origin of basalt; III, Petrogenesis of the Mauna Ulu eruption, Kilauea, 1969–1971. Contrib Mineral Petrol 88(1–2):24–35

Hofmann AW (1988), Chemical differentiation of the earth: the relationship between mantle, continental crust, and oceanic crust. Earth Planet Sci Lett 90:297–314

Hofmann AW (1997), Mantle geochemistry; the message from oceanic volcanism. Nature 385(6613):219–229

Honnorez J, Mevel C, Honnerez-Guerstein BM and Tomschi HP (1990), Mineralogy and chemistry of sulfide deposits drilled from hydrothermal mound of the snake pit active field, MAR. In: Detrick, R, Honnorez J, Bryan WB, Juteau, T, et al (eds), Proceedings of the Ocean Drilling Program, Scientific Results, Vol 106/109: U.S. Government Printing Office, pp 145–162, Washington

Huang S, Frey FA (2003), Trace element abundances of Mauna Kea basalt from Phase 2 of the Hawaiian Scientific Drilling Project: petrogenetic implications of correlations with major element content and isotopic ratios. Geochem Geophys, Geosys 4(6):8711, doi, 1029/2002 GC000322

Jackson MC, Wilmoth RA, and Frey FA (1999), Geology and petrology of basaltic lavas and dikes of the Koolau Volcano in the Trans-Koolau exploratory tunnels, Oahu, Hawaii. Bull Volcan 60:381–401

Kelemen PB (1986), Assimilation of ultramafic rock in subduction-related magmatic arcs. J Geol 94(6):829–843

Kogiso T, Hirschmann MM, Reiners PW (2004), Length scales of mantle heterogeneities and their relationship to ocean island basalt geochemistry, Geochim Cosmochim Acta 68(2):345–360, doi, 10.1016/S0016-7037(03)00419-8

Kurz MD, Kenna TC, Kammer DP, Rhodes JM, Garcia MO (1995), Isotopic evolution of Mauna Loa volcano: a view from the submarine southwest rift Mauna Loa: A Decade Volcano. In: Rhodes JM, Lockwood JP (eds) Mauna Loa Revealed. Geophys Monogr Ser 92; 289–306

Lassiter JC, Hauri EH (1998), Osmium-iosotope variations in Hawaiian lavas: Evidence for recycled oceanic lithosphere in the Hawaiian plume. Earth Planet Sci Letts 164:483–496

Leeman WP, Gerlach DC, Garcia MO, West HB (1994). Geochemical variations in lavas from Kahoolawe volcano, Hawaii: evidence for open system evolution of plume-derived magmas. Contrib Mineral Petrol 116:62–77

Li X, Kind R, Yuan X, Wölbern I, Hanka W (2004), Rejuvenation of the lithosphere by the Hawaiian plume. Nature 427:827–829 doi:10.1038/nature02349

Norman MD, Garcia MO (1999), Primitive magmas and source characteristics of the Hawaiian Plume; petrology and geochemistry of shield picrites. Earth Planet Sci Letts 168:27–44

Norman MD, Garcia MO and Bennett VC (2004), Rhenium and chalcophile elements in basaltic glasses from Ko'olau and Moloka'i volcanoes: Magmatic outgassing and composition of the Hawaiian plume. Geochim Cosmochim Acta 68(18):3761–3777, doi: 10.1016/j.gca.2004.02.025

Patino LC, Carr MJ, Feigenson MD (2000), Local and regional variations in Central American arc lavas controlled by variations in subducted sediment input. Contrib Mineral Petrol 138(3):265–283

Pertermann M, Hirschmann MM (2003a), Anhydrous partial melting experiments on MORB-like eclogite: Phase reactions, phase compositions and mineral-melt partitioning of major elements at 2–3 GPa. J Petrol 44(12):2173–2201

Pertermann M and Hirschmann MM (2003b), Partial melting experiments on a MORB-like pyroxenite between 2 and 3 GPa; constraints on the presence of pyroxenite in basalt source regions from solidus location and melting rate. J Geophys Res 108(B2):2125, doi: 10.1029/2000JB000118

Pertermann M, Hirschmann MM, Hametner K, Gunther D, Schmidt MW (2004), Experimental determination of trace element partitioning between garnet and silica-rich liquid during anhydrous partial melting of MORB-like eclogite. Geochem Geophys, Geosyst, 5, Q05A01, doi:10.1029/2003GC000638

Pietruszka AJ, Garcia MO (1999), A rapid fluctuation in the mantle source and melting history of Kilauea Volcano inferred from the geochemistry of its historical summit lavas (1790–1982): J Petrol 40(8):1321–1342

Plank T, Langmuir CH (1998), The chemical composition of subducting sediment and its consequences for the crust and mantle. Chem Geol 145(3–4):325–394

Plank T (2005), Constraints from Thorium/Lanthanum on Sediment Recycling at Subduction Zones and the Evolution of the Continents. J Petrol doi:10.1093/petrology/egi005

Plank T, Balzer V, Carr M (2002), Nicaraguan volcanoes record paleoceanographic changes accompanying closure of the Panama gateway. Geology 30(12):1087–1090

Press WH, Teukolsky SA, Vetterling WT, Flannery BP (1992), Numerical Recipes in C, 2nd edn. Cambridge University Press, New York, pp 994

Putirka K (1999), Melting depths and mantle heterogeneity beneath Hawaii and the East Pacific Rise; constraints from Na/Ti and rare earth element ratios. J Geophys Res 104(2):2817–2829

Quane SL, Garcia MO, Guillou H, Hulsebosch TP (2000), Magmatic history of the East Rift Zone of Kilauea Volcano, Hawaii based on drill core from SOH 1. J Volcanol Geotherm Res 102(3–4):319–338

Ray JS, Martin MW, Veizer J, Bowring SA (2002), U-Pb zircon dating and Sr isotope systematics of the Vindhyan Supergroup, India. Geology 30(2):131–134

Reiners PW (2002), Temporal-compositional trends in intraplate basalt eruptions: Implications for mantle heterogeneity and melting processes, Geochem Geophys Geosyst 3(2) 10.1029/2001GC000250

Rhodes JM, Hart SR (1995), Episodic trace element and isotopic variation in historical Mauna Loa lavas. In: Rhodes JM, Lockwood JP (eds) Mauna Loa Revealed, Geophys Monogr Ser 92. 263–288

Rhodes JM (1996), Geochemical stratigraphy of lava flows sampled by the Hawaii Scientific Drilling Project. J Geophys Res 101:11,729–11,746

Rhodes JM, Vollinger MJ (2004), Composition of basaltic lavas sampled by phase-2 of the Hawaii Scientific Drilling Project: Geochemical stratigraphy and magma types. Geochem Geophys Geosyst, 5, Q03G13, doi:10.1029/2002GC000434

Ribe NM, Christensen UR (1999), The dynamical origin of Hawaiian volcanism. Earth Planet Sci Lett 171(4):517–531

Roden MF, Trull T, Hart SR, Frey FA (1994), New He, Sr, Nd and Pb isotopic constraints on the constitution of the Hawaiian plume: results from Koolau Volcano, Oahu, Hawaii. Geochim Cosmochim Acta 58:1431–1440

Salters VJM (1996), The generation of mid-ocean ridge basalts from the Hf and Nd isotope perspective. Earth Planet Sci Letts 141:109–123

Salters VJM, Longhi J (1999), Trace element partitioning during the initial stages of melting beneath mid-ocean ridges. Earth Planet Sci Letts 166:15–30

Seitz H-M, Altherr R, Ludwig T (1999), Partitioning of transition elements between orthopyroxene and clinopyroxene in peridotitic and websteritic xenoliths; new empirical geothermometers. Geochim Cosmochim Acta 63(23–24):3967–3982

Sharp WD, Renne PR (2005), ^{40} Ar/^{39} Ar dating of core recovered by the Hawaii Scientific Drilling Project (Phase 2) Hilo, Hawaii, Geochem Geophys Geosyst, 6,Q04G17, doi:10.1029/2004GC000846

Shinozaki K, Ren Z-Y, Takahashi E (2002), Geochemical and petrological characteristics of Nuuanu and Wailau landslide blocks. In: Takahashi E, Lipman PW, Garcia MO, Naka J, Aramaki S (eds) Hawaiian volcanoes; deep underwater perspectives, Geophys Monogr Ser 128: 297–310

Sobolev AV, Hofmann AW, Nikogosian IK (2000), Recycled oceanic crust observed in ghost plagioclase within the source of Mauna Loa lavas. Nature 404:986–990

Sobolev AV, Hofmann AW, Sobolev SV, Nikogosian IK (2005), An olivine-free mantle source of Hawaiian shield basalts. Nature 434:590–597, doi: 10.1038/nature03411

Stolper E, Sherman S, Garcia M, Baker M, Seaman C (2004), Glass in the submarine section of the HSDP2 drill core, Hilo, Hawaii. Geochem Geophys Geosys, 5, Q07G15, doi:10.1029/2003GC000553

Takahashi E, Nakajima K, Wright TL (1998), Origin of the Columbia River basalts; melting model of a heterogeneous plume head. Earth Planet Sci Letts 162:63–80

Takahashi E, Nakajima K (2002), Melting process in the Hawaiian Plume; an experimental study. In: Takahashi E, Lipman PW, Garcia MO, Naka J, Aramaki S (eds) Hawaiian volcanoes; deep underwater perspectives Geophys Monogr Ser 128:403–418

Tanaka R, Nakamura E, Takahashi E (2002), Geochemical evolution of Koolau Volcano, Hawaii. In: Takahashi E, Lipman PW, Garcia MO, Naka J, Aramaki S (eds) Hawaiian volcanoes; deep underwater perspectives. Geophys Monogr Ser 128:311–332

Thompson G, Humphris SE, Schroeder B, Sulanowska M, Rona PA (1988), Active vents and massive sulfides at 26°N (TAG) and 23°N (Snakepit) on the mid-Atlantic ridge. Can Mineral 26:697–711

Tu G, Zhao Z, Qiu Y (1985), Evolution of Precambrian REE mineralization. Precamb Res 27:131–151

van Westrenen W, Blundy J, Wood B (1999), Crystal-chemical controls on trace element partitioning between garnet and anhydrous silicate melt. Am Mineral 84:838–847

van Westrenen W, Blundy JD, Wood BJ (2001), High field strength element/rare earth element fractionation during partial melting in the presence of garnet; implications for identification of mantle heterogeneities, Geochem Geophys, Geosys 2(7):doi:10.1029/2000GC000133

Wagner TP, Grove TL (1998), Melt/harzburgite reaction in the petrogenesis of tholeiitic magma from Kilauea Volcano, Hawaii. Contrib Mineral Petrol 131(1):1–12

Walter MJ (1998), Melting of garnet peridotite and the origin of komatiite and depleted lithosphere. J Petrol 39(1):29–60

Yaxley GM, Green DH (1998) Reactions between eclogite and peridotite: mantle refertilisation by subduction of oceanic crust, Schweiz. Mineral Petrogr Mitt 78:243–255

Yogodzinski GM, Kay RW, Volynets ON, Koloskov AV, Kay SM (1995), Magnesian andesite in the western Aleutian Komandorsky region; implications for slab melting and processes in the mantle wedge. Geol Soc Am Bull 107(5):505–519

Zhong S, Watts AB (2002), Constraints on the dynamics of mantle plumes from uplift of the Hawaiian Islands. Earth Planet Sci Letts 203:105–116